Received: Added at production | Revised: Added at production | Accepted: Added at production

DOI: xxx/xxxx

RESEARCH ARTICLE

Multi-stage Stochastic Programming for Integrated Network Optimization in Hurricane Relief Logistics and Evacuation Planning

Sudhan Bhattarai | **Yongjia Song**

Department of Industrial Engineering, Clemson University, South Carolina, United States

Correspondence
Yongjia Song
Email: yongjis@clemson.edu

Abstract

In this paper, we study the integrated hurricane relief logistics and evacuation planning (IHRLEP) problem, integrating hurricane evacuation and relief item pre-positioning operations that are typically treated separately. We propose a fully adaptive multi-stage stochastic programming (MSSP) model and solution approaches based on two-stage stochastic programming (2SSP). Utilizing historical forecast errors modeled using the auto-regressive model of order one, we generate hurricane scenarios and approximate the hurricane process as a Markov chain, and each Markovian state is characterized by the hurricane's location and intensity attributes. We conduct a comprehensive numerical experiment based on case studies motivated by Hurricane Florence and Hurricane Ian. Through the computational results, we demonstrate the value of fully adaptive policies given by the MSSP model over static ones given by the 2SSP model in terms of the out-of-sample performance. By conducting an extensive sensitivity analysis, we offer insights into how the value of fully adaptive policies varies in comparison to static ones with key problem parameters.

KEYWORDS

Hurricane evacuation, disaster relief logistics network optimization, multi-stage stochastic programming, Markov chain

1 | INTRODUCTION

Hurricanes are among the deadliest natural disasters in the United States. Hurricane Laura [34] in 2020 caused 81 deaths and an estimated 23.3 billion US dollars worth of infrastructure damage, while Hurricane Ian 2022 caused 150 deaths and an estimated 112 billion US dollars [13]. People under the threat of a hurricane may opt to evacuate to shelters because of personal safety concerns, power outages, and flooding [6]. While most evacuees shelter in hotels or resort to families and friends, on average around 11% evacuees from the potential affected areas, which we refer to as demand points (DPs), evacuate to public shelters that we refer to as shelter points (SPs) [6]. In the meantime, relief items (such as food, water, and medical kits) are prepositioned at the SPs, which are typically shipped from the main distribution center (MDC) or an incident support base established by the Federal Emergency Management Agency (FEMA) for the hurricane event. Clearly, the operations of evacuation and the relief item pre-positioning at the SPs must be coordinated to ensure the well-being of the evacuees at the SPs. In this paper, we study an integrated hurricane relief logistics and evacuation planning (IHRLEP) problem.

The evacuation operation is a multi-period process. A timely evacuation plan is crucial to ensure sufficient time for the evacuation operation, which can last two to three days. After the hurricane's formation, at a frequency of every six hours, the National Hurricane Center (NHC) issues a hurricane forecast advisory up to the next five days, including the hurricane's projected track (longitude, latitude) and intensity (wind speed). The projected landfall location of an impending hurricane determines what we refer to as the risk zone. Inside the risk zone, the evacuation demand from the DPs, i.e., the number of evacuees, depends on the evacuation behavior, such as the socioeconomic background and risk attitudes of the affected

population, under the projected hurricane's attributes [10]. The challenge here is that the hurricane forecast is imperfect and subject to forecast errors, which imposes uncertainty on the hurricane's future attributes and hence the corresponding demand. In this case, a deterministic optimization model may be insufficient to address the challenges brought by the various sources of uncertainty in this process. It is preferred to utilize models and approaches based on optimization under uncertainty.

One key consideration in developing these models and approaches is to balance between the (evacuation) operation lead time and the hurricane's forecast uncertainty. The evacuation plans made in earlier stages of the hurricane's evolution may suffer from higher potential forecast errors (FEs). For example, they may lead to a significant mismatch between the estimated demand of relief items and the actual realized demand. On the other hand, despite the fact that evacuation plans made with a more accurate forecast as the hurricane moves closer to its landfall can address potential demand mismatch, it may suffer from the insufficient amount of time to effectively execute the evacuation. Therefore, it is important to address the challenge in the timing of decision making in logistics and evacuation planning.

Multi-stage stochastic programming (MSSP) models have shown to be effective in sequential decision-making under uncertainty, especially in applications that arise in large-scale network systems such as supply chain and energy [52, 35]. MSSP models are fully adaptive in the sense that the decisions at each stage are made according to the realized system state at that point. Despite its flexibility and adaptability, it is computationally challenging to obtain an optimal decision policy for the MSSP model [42]. Alternatively, one may consider a static decision policy based on a two-stage stochastic programming (2SSP) approximation to the MSSP. A 2SSP model solved at the beginning of the planning horizon may be lack of flexibility in adapting its decisions according to uncertainty realization. This shortcoming can be partially addressed by implementing the 2SSP model in a rolling-horizon (RH) procedure [23]. In this procedure, we sequentially solve a 2SSP model as the so-called stochastic look-ahead model (SLAM) at every stage the planning horizon, but only implement the decisions that apply to the current stage.

In this paper, we formulate a multi-period IHRLEP problem as an MSSP by integrating the evacuation decisions relief logistics decisions to minimize the overall expected operational over the network. The contribution of our paper is three-hold. First, we propose a fully adaptive MSSP model to formulate the IHRLEP and demonstrate its advantage over a static policy given by a 2SSP model through numerical experiments. Second, we demonstrate how to model the time-dependent evolution of forecast uncertainty based on historical hurricane forecast errors and how to integrate this information within an MSSP model. Third, we discuss two different settings of the hurricane process based on whether or not the hurricane's landfall time is random or deterministic, and demonstrate the value of the fully adaptive policy over the static policy using realistic case studies inspired by Hurricane Florence and Ian.

The remainder of the paper is structured as follows: Section 2 provides a brief literature review. Section 3 describes the mathematical formulations of the MSSP model and its 2SSP approximation for the IHRLEP problem. Section 4 presents the solution methods used for solving MSSP and 2SSP models. Section 5 presents the experimental setup, followed by the presentation of numerical results and discussions based on two case studies in Section 6. Section 7 summarizes the paper with some concluding remarks.

2 | LITERATURE REVIEW

In this paper, we delve into an integrated decision making problem where evacuation operations and their impacts on the demand for relief items are closely intertwined. It is noteworthy that the existing body of literature primarily treats evacuation and relief logistics as distinct and separate challenges. Furthermore, the few investigations pertaining to the integrated problem typically confine themselves to a single-period deterministic planning model. In the subsequent sections, we first review studies focusing on evacuation and relief logistics separately, followed by a discussion of recent literature dedicated to the integrated problem.

2.1 | Disaster relief logistics planning

Our paper directly contributes to the issue of disaster relief logistics planning in terms of relief item pre-positioning. In a survey paper conducted by [41], the authors underscore that existing research predominantly concentrates on traditional supply-side cost-related objectives. They advocate for future research efforts to bridge this gap by integrating demand-side costs into the model objectives. Additionally, they emphasize the importance of exploring research avenues related to pre-positioning as a

risk mitigation strategy and the synergistic approach to addressing pre-positioning challenges within the context of disaster preparedness.

Stochastic optimization models for relief pre-positioning

Due to the various sources of uncertainty in disaster relief logistics, two-stage stochastic optimization models have been popular in this context. For example, studies by [32] and [8] have provided insights into relief item pre-positioning under uncertain supply and demand for relief items. [15] introduced a rolling horizon method that employs a two-stage mixed-integer programming model to address pre-positioning. They focused on minimizing the logistics and social costs associated with unsatisfied demand under hurricane uncertainty. [47] developed a two-stage robust optimization model specifically tailored to hurricane relief logistics, accounting for demand uncertainty tied to hurricane severity and logistics pre-positioning disruptions during landfall. [51] expanded upon hurricane relief logistics by incorporating social costs in a two-stage robust optimization framework. They explored the trade-offs between early pre-positioning and waiting for hurricane evolution. [22] addressed pre-positioning in a two-echelon logistics network with a two-stage location allocation model, ensuring demand satisfaction across multiple earthquake scenarios.

In addition to two-stage stochastic optimization, other optimization models and solution approaches have been proposed in the literature. For example, [44] investigated a chance-constrained stochastic programming model, focusing on maximizing pre-positioning response within budget constraints in humanitarian operations. [48] introduced a two-stage risk-averse distributionally robust optimization (DRO) approach. Their model integrated facility location and multi-commodity flow considerations, minimizing first-stage costs related to facility placement and relief purchases, while also accounting for worst-case second-stage relief supply costs. [40] studied the timing of preparedness activities. Their analysis considered logistics pre-positioning and response costs, as well as the minimum travel time required for transporting relief items to demand zones. [45] proposed a multi-tier logistics network model with random hurricane landfall times. Pre-positioning was carried out across three tiers, with uncertain demand realized during the landfall period. [21] and [7] delved into the optimization of pre-positioning specific resources, such as diesel fuel and pharmaceutical supplies, within emergency relief operations.

These studies collectively contribute to the development of effective strategies for pre-positioning relief items, taking into account diverse factors, uncertainties, and optimization objectives. However, these decisions do not take into account the decisions made in evacuation operation. The stochastic demand data for relief items in these studies is not influenced by the evacuation decisions. In our study, we make decisions for the pre-positioning and supply of relief items in coordination with the evacuation decisions.

2.2 | Hurricane evacuation planning

Various dynamic and stochastic models have been utilized in evacuation planning to optimize dynamic evacuation decision policies. For instance, [25] discussed the application of a genetic algorithm to identify feasible solutions for a multi-period evacuation network, encompassing different modes of transportation from evacuation zones to shelters. Similarly, [31] addressed the capacitated network flow problem to maximize the total number of evacuations within a short evacuation window. While these studies underscore the significance of dynamic evacuation planning as a multi-period endeavor, they often overlook the uncertainty associated with evacuation start times and the unfolding of demand throughout the planning horizon. Partially addressing this gap, [39] proposed a dynamic, forecast-driven Markov decision process model aimed at determining optimal evacuation timings. However, their stochastic model primarily focuses on identifying the evacuation start time and does not integrate seamlessly with evacuation and relief logistics decisions.

In the literature of stochastic programming and its applications, models for evacuation have been well-studied due to their dynamic and uncertain nature. For example, [50] formulated the evacuation problem with uncertainty in travel time and capacity of evacuation routes in a scenario based stochastic programming framework. The two-stage model discussed by [11] considered the uncertainty in evacuation demand and disruptions in road caused by the disaster. Moreover, [9] developed a bi-level stochastic optimization model that focuses on determining the appropriate number of evacuees and their evacuation routes. Further expanding on these ideas, [49] proposed a two-stage model that integrates strategic decisions both before and after a disaster, aiming to minimize travel costs. This model particularly considers the effects of disruptions on the transportation network, which introduces uncertainties in travel time and the routes' evacuation capacities. [18] proposed an MSSP model, aiming to optimize the timing of evacuation orders and the travel time for evacuees. Their model considers evacuee behavior

and hazard assessment as critical factors. A risk-averse two-stage model with chance constraints was proposed by [30] that addresses demand uncertainty in evacuation while minimizing the evacuation time.

Despite the extensive studies on optimizing evacuation decisions, most of the literature that focused on evacuation problem does not consider the concurrent task of providing the evacuees with relief items, which is directly affected by the evacuation decisions. The evacuation problem alone accounts for the timely evacuation and safety of the evacuees. However, integrating relief logistics together helps decision makers to efficiently pre-position the relief items to reduce the logistics cost and social cost in providing relief items to evacuees at SPs. In our paper, we extend these concepts by factoring in demand uncertainty and examining how evacuation decisions influence the efficacy of the relief logistics network.

2.3 | Integrated disaster relief logistics and evacuation planning

Among a few recent papers in the literature that consider the integrated evacuation and relief logistics problem, [46] proposed a three-tier network consisting of a relief logistics network and an evacuation network in a single period planning horizon. Their multi-objective model in a deterministic setting focused on minimizing the logistics and fixed cost. Specifically, their objective constituted the minimization of maximum travel distance for evacuees, cost of relief transportation, and cost related with opening SPs and distribution centers. Hurricane uncertainty in an integrated model was discussed by [17]. The authors incorporated uncertainty in demand realization, as a result of the uncertain hurricane process on the evacuation side of the network and the impact of associated evacuation decisions on the relief logistics side of the network into a two-stage stochastic programming model that minimizes the expected logistics cost of the entire network and the cost of the worst case scenario. This paper is the closest to our paper in the sense that it studies the impact of evacuation decisions on the relief logistics in case of hurricane uncertainty. However, this study is limited to a single period planning. Our study fills this gap by proposing an integrated framework in a multi-period setting.

In this paper, we combine the evacuation and relief logistics decisions in a multi-period IHRLEP and propose fully adaptive, static, and dynamic policies to solve the problem. We demonstrate the value of a fully adaptive policy over a static policy and analyze the effect of decisions made on the evacuation side to the relief item pre-positioning decisions.

3 | STOCHASTIC PROGRAMMING MODELS AND SOLUTION APPROACHES

In this section, we describe the stochastic programming models for the IHRLEP to minimize the total expected evacuation and logistics cost over the planning horizon. We begin by defining the following sets:

Sets

- I Set of DPs.
- J Set of SPs.
- $\mathcal{T}$ Set of time periods in the planning horizon: $\{1, 2, \ldots, T\}$.

We use index $j = 0$ to represent the MDC and set $J \cup \{0\}$ to represent the set of all facilities on the logistics side of the network, i.e., the SPs and the MDC. The notation for the parameters of the IHERLP problem is presented as follows:

Parameters

- D_i The total population of location $i \in I$ before evacuation.
- q_j Maximum number of evacuees allowed at SP $j \in J$.
- c_j^F One-time setup cost of SP $j \in J$ upon activation.
- c_j^f Keep-up cost (per period) of an active SP $j \in J$.
- $d_{i,j}$ The distance between location $i \in I \cup J \cup \{0\}$ and location $j \in I \cup J \cup \{0\} \setminus \{i\}$
- $c_{i,j}^E$ Unit evacuation cost from DP $i \in I$ to SP $j \in J$.
- $c_{j',j}^R$ Unit transportation cost of relief items from $j' \in J \cup \{0\}$ to SP $j \in J$.
- c_i^{PE} Unit penalty cost for unsatisfied evacuation demand at DP $i \in I$.
- c_j^G Unit cost of *emergency* relief items shipped to SP $j \in J$.
- c^P Unit procurement cost of relief items from the MDC to SPs.
- c_j^H Unit cost for *unused* relief items to be shipped out of SP $j \in J$.
- c_j^{InvR} Unit inventory cost of relief items in SP $j \in J$ per period.
- c_j^{InvE} Unit operating cost of SP $j \in J$ (per evacuee) per period.
- ϕ Amount of relief items needed per evacuee per period.

With the sets and parameters stated above, we continue by defining a fully adaptive MSSP model. We note that because of the full adaptability, we refer to terms "stage" and "period" interchangeably in this model.

3.1 | A multi-stage stochastic programming model

To start, we follow [43] and provide a nested formulation of a generic risk-neutral MSSP model in (1). At each period $t \in \mathcal{T}$, the (x_t, y_t) pair represents the state and local decision variables, respectively, which will be explained in detail later in the context of the IHRLEP problem. The random vector ξ_t represents the realization of the underlying stochastic process at $t \in \mathcal{T}$, and $\xi_{[t]}$ represents the realized history of this stochastic process up to time t, i.e., $\{\xi_1, \cdots, \xi_t\}$. The feasible set X_t at $t \in \mathcal{T}$ depends on the state variable from $t-1$, i.e., x_{t-1}, and random vector ξ_t. As a convention in MSSP, the initial condition x_0 is known and ξ_1 is deterministic.

$$\begin{aligned} &\min_{(x_1,y_1)\in X_1(x_0,\xi_1)} f_1(x_1,y_1) \\ &+ \mathbb{E}_{|\xi_{[1]}}\left[\min_{(x_2,y_2)\in X_2(x_1,\xi_2)} f_2(x_2,y_2) + \mathbb{E}_{|\xi_{[2]}}\left[\cdots + \mathbb{E}_{|\xi_{[T-1]}}\left[\min_{(x_T,y_T)\in X_T(x_{T-1},\xi_T)} f_T(x_T,y_T)\right]\right]\right] \end{aligned} \tag{1}$$

In general, the stochastic process denoted by $\{\xi_t\}_{t\in\mathcal{T}}$ is typically represented in the form of a scenario tree, possibly after certain discretization. However, the size of the scenario tree grows exponentially fast as the number of stages increases. In this paper, we resort to a Markov chain (MC) approximation of the underlying stochastic process, which is validated through historical data for the IHRLEP problem as we demonstrate in Section 5. This makes it computationally much more viable to solve formulation (1). Before we proceed, we note that such a Markovian assumption allows us to rewrite (1) as:

$$\begin{aligned} &\min_{(x_1,y_1)\in X_1(x_0,\xi_1)} f_1(x_1,y_1) \\ &+ \mathbb{E}_{|\xi_1}\left[\min_{(x_2,y_2)\in X_2(x_1,\xi_2)} f_2(x_2,y_2) + \mathbb{E}_{|\xi_2}\left[\cdots + \mathbb{E}_{|\xi_{T-1}}\left[\min_{(x_T,y_T)\in X_T(x_{T-1},\xi_T)} f_T(x_T,y_T)\right]\right]\right], \end{aligned} \tag{2}$$

where random vector ξ_t represents the realization of the Markovian state at period t.

The task of finding an optimal decision policy for (2) can be accomplished by a stage-wise decomposition framework, in which the sum of the immediate cost and the expected future cost at every stage t for each Markovian state ξ_t is minimized. Specifically, for each Markovian state ξ_t in each stage $t \in \mathcal{T}$, we define the associated subproblem using dynamic programming equations below:

$$Q_t(x_{t-1}, \xi_t) = \min_{x_t, y_t} f_t(x_t, y_t) + \mathcal{Q}_{t+1}^{\xi_t}(x_t) \tag{3a}$$

$$\text{s.t. } \tilde{A}_t^{\xi_t} x_t + \tilde{H}_t^{\xi_t} y_t \geq \tilde{b}_t^{\xi_t} + \tilde{B}_t^{\xi_t} x_{t-1}, \tag{3b}$$

where $Q_t(\cdot, \xi_t)$ is called the *cost-to-go (CTG) function* at stage t and $\mathcal{Q}_{t+1}^{\xi_t}(\cdot) := \mathbb{E}_{\xi_{t+1}|\xi_t}[Q_{t+1}(\cdot, \xi_{t+1})]$ is called the *expected CTG function*. Since $t = T$ is the terminal stage, the expected CTG function $\mathcal{Q}_{T+1}^{\xi_T}(\cdot) \equiv 0$ for any state ξ_T in the terminal stage T. Each Markovian state ξ_t corresponds to a set of parameters $\xi_t := \{\tilde{A}_t^{\xi_t}, \tilde{H}_t^{\xi_t}, \tilde{b}_t^{\xi_t}, \tilde{B}_t^{\xi_t}\}$ used in (3). At a stage t, given values of state variables x_{t-1} and a Markovian state ξ_t, the stage-t problem is optimized to minimize the immediate cost $f_t(x_t, y_t)$ plus the expected future cost that is represented by the expected CTG function $\mathcal{Q}_{t+1}^{\xi_t}(x_t)$.

To formulate the MSSP model for the IHRLEP problem, we describe the specific characteristics of the decision variables, objective function, constraints, and the underlying MC model. In our MSSP model for IHRLEP, the objective function $f_t(\cdot)$ is a linear function of x_t and y_t, and matrices A_t, H_t and vectors b_t are deterministic for each $t \in \mathcal{T}$. The uncertain parameters, which correspond to the evacuation demand realization at each period $t \in \mathcal{T}$ (as a result of the Markovian state ξ_t of hurricane), is part of $\tilde{B}_t^{\xi_t}$.

Markov chain model

As we demonstrate in more details in Section 5, the Markovian state ξ_t includes the hurricane track and intensity information and we assume that the demand realization at t can be computed according to a given mapping from the Markovian state. More specifically, the Markovian states associated with the hurricane are categorized into *absorbing* states and *transient* states. We assume that the absorbing states are of two types: final-stage states and landfall states. The final-stage states include all the states at $t = T$, while the landfall states are the states that correspond to the hurricane's landfall prior to reaching the final stage T. We will elaborate on this later as we describe the two different cases associated with deterministic versus stochastic

landfall time. All other states, i.e., the states that are not absorbing, are transient states. The transition probabilities $p_{\xi_t,\xi_{t+1}}$ from Markovian state ξ_t to ξ_{t+1} for each pair of (ξ_t, ξ_{t+1}) are known. In our numerical experiments, these transition probabilities are estimated from historical data using certain discretization techniques, as will be shown in Section 5. Given a hurricane state ξ_t, we let D_{i,ξ_t} denote the associated demand at DP $i \in I$, which corresponds to evacuation needs in DP i at period t, represented as a fraction of the remaining vulnerable population in this DP. We assume that D_{i,ξ_t} can be computed based on a given mapping estimated from empirical evacuation behavioral studies [6, 24]. We note that the evacuation demand being modeled as a fraction of the remaining vulnerable population at DPs is a key characteristics of our model. As a result of this, the unfulfilled demand at a period does not mean a complete disposal of the evacuees from the system as they can be accounted for in later periods.

Decision variables

Our proposed MSSP formulation involves both continuous and integer decision variables. The integer decision variables are associated with the status of the activation of SPs. In practice, public shelters (which we model as SPs) are activated based on hurricane forecasts [1]. We make the following assumption about the activation of SPs.

Assumption 1. The SPs need to be activated to use and they stay open until the end of the planning horizon once activated.

Ideally, the decision maker may choose to implement an adaptive SP activation decision policy as hurricane uncertainty unfolds since the fixed cost to activate and maintain SPs can be very high. However, this would result in a fully adaptive mixed integer MSSP model, which is notoriously challenging to solve [53]. Furthermore, SP facilities include a variety of public building such as schools and hospitals [1]. The lead time for shelter opening can be long as the shelter preparation may require significant amount of time in advance. Based on these considerations, we limit these integer decision variables to the first stage only in our MSSP formulation with the following assumption:

Assumption 2. The activation of SPs must be made at the beginning of the planning horizon, constituting the first-stage decisions regarding SPs opening.

The decision variables for each stage-t problem of the proposed MSSP model for the IHRLEP problem are defined on Table 1. The decision variables $e_{j,t}/e_{i,t}$ and $\ell_{j,t}$ represent the number of evacuees and relief items, respectively, at their corresponding locations. These variables are the state variables as they are carried over to the subsequent periods in the planning horizon. In what follows, we denote the vectors of all state variables and their corresponding values at a stage $t \in \mathcal{T}$ for brevity by X_t and $\hat{X}_t$, respectively. At the start of the planning horizon, the initial conditions of the state variables are defined as follows: $\hat{e}_{j,0} = 0,\ \forall j \in J,\ \hat{e}_{i,0} = \bar{D}_i,\ \forall i \in I,\ \hat{\ell}_{j,0} = 0,\ \forall j \in J$. All other variables are local variables that only participate in the stage-t problem associated with Markovian state ξ_t. An illustrative example of the decision variables is presented in Figure A1 in the Appendix.

TABLE 1 The decision variables for each stage-t problem of the proposed MSSP model.

$z_j \in \{0, 1\}$	Whether or not SP $j \in J$ is open
$\ell_{j,t}$	Inventory level of relief items at $j \in J$ at the end of period t.
$e_{i,t}/e_{j,t}$	Number of evacuees at location $i \in I/j \in J$ at the end of period t.
$y_{i,j,t}$	Number of people to evacuate from $i \in I$ to $j \in J$ at period t.
$u_{i,t}$	Unmet evacuation demand at $i \in I$ at period t.
$x_{j',j,t}$	Amount of relief items shipped from $j' \in J \cup \{0\} \setminus \{j\}$ to SP $j \in J$ at period t.
$g_{j,t}/h_{j,t}$	Amount of *emergency*/*unused* relief items shipped to/from $j \in J$ at period t.

In terms of the periods, we consider each period to be 12 hours long which is motivated by the NHC's point forecast intervals [2]. We note that one period in our model is sufficient to carry out the transportation of relief items and evacuees between any pair of locations, which is stated by Assumption 3. This allows us to model the underlying optimization problem using a multi-period network flow formulation instead of the more complicated time-indexed network flow formulation.

Assumption 3. The transportation of relief items and evacuees between any pair of locations can be completed within one period.

3.1.1 | The first-stage problem

The first-stage problem of the proposed MSSP model includes both the binary decision variables on SP activation and the continuous decision variables on logistics operation, which is defined as follows:

$$Q_1 = \min \sum_{j\in J}(c_j^F + c_j^f \times |T|)z_j + \sum_{j\in J}(c^P + c_{0,j}^R)x_{0,j,1} + \sum_{j'\in J}\sum_{j\in J} c_{j',j}^R x_{j',j,1} + \sum_{i\in I}\sum_{j\in J} c_{i,j}^E y_{i,j,1} + \sum_{j\in J} c_j^G g_{j,1} + \sum_{j\in J} c_j^H h_{j,1} + \sum_{i\in I} c_i^{PE} u_{i,1} + \sum_{j\in J} c_j^{InvE} e_{j,1} + \sum_{j\in J} c_j^{InvR}\ell_{j,1} + \mathcal{Q}_2^{\xi_1}(X_1) \tag{4a}$$

$$\text{s.t.} \sum_{j\in J} y_{i,j,1} + u_{i,1} = D_{i,\xi_1}\hat{e}_{i,0},\ \forall i \in I \tag{4b}$$

$$\hat{e}_{i,0} - \sum_{j\in J} y_{i,j,1} = e_{i,1},\ \forall i \in I \tag{4c}$$

$$\hat{e}_{j,0} + \sum_{i\in I} y_{i,j,1} = e_{j,1},\ \forall j \in J \tag{4d}$$

$$e_{j,1} \le q_j z_j,\ \forall j \in J \tag{4e}$$

$$\ell_{j,1} \le \phi q_j z_j,\ \forall j \in J \tag{4f}$$

$$\hat{\ell}_{j,0} + g_{j,1} - \phi e_{j,1} \le \phi q_j z_j,\ \forall j \in J \tag{4g}$$

$$\hat{\ell}_{j,0} + x_{0,j,1} + \sum_{j'\in J, j'\neq j} x_{j',j,1} - \sum_{j'\in J, j\neq j'} x_{j,j',1} - \phi e_{j,1} + g_{j,1} - h_{j,1} = \ell_{j,1},\ \forall j \in J \tag{4h}$$

$$\sum_{j'\in J, j\neq j'} x_{j,j',1} \le \hat{\ell}_{j,0} + g_{j,1} - \phi e_{j,1},\ \forall j \in J \tag{4i}$$

$$u_{i,1}, e_{i,1} \ge 0,\ \forall i \in I; e_{j,1}, \ell_{j,1}, h_{j,1}, g_{j,1} \ge 0,\ \forall j \in J \tag{4j}$$

$$y_{i,j,1} \ge 0,\ \forall i \in I,\ \forall j \in J; x_{j,j',1} \ge 0,\ \forall j \in J \cup \{0\},\ \forall j' \in J : j \neq j' \tag{4k}$$

$$z_j \in \{0,1\},\ \forall t \in \mathcal{T},\ \forall j \in J, \tag{4l}$$

where $\mathcal{Q}_2^{\xi_1}(X_1)$ is the expected CTG function at $t = 2$, which is defined as:

$$\mathcal{Q}_2^{\xi_1}(X_1) = \mathbb{E}_{\xi_2|\xi_1}\left[Q_2(X_1, \xi_2)\right] = \sum_{\xi_2\in\Xi_2} p_{\xi_1,\xi_2} Q_2(X_1, \xi_2),$$

where p_{ξ_1,ξ_2} gives the transition probability from ξ_1 to ξ_2.

In the objective function (4a), the first term represents the one-time fixed cost and the per-period keep-up cost associated with the activation of SPs, respectively. The second term represents the overall cost linked to procuring relief items at the MDC and shipping to SPs. The third and fourth terms present the cost related to the transportation of relief items among SPs and the transportation of evacuees from DPs to SPs, respectively. The fifth and sixth terms represent the emergency transportation cost of relief items and the salvage value for unused relief items, respectively. The seventh term represents the penalty cost incurred due to unmet evacuation demand. The eighth and ninth terms account for the inventory costs incurred in holding evacuees and relief items, respectively. The last term represents the expected CTG function at $t = 2$ as indicated above.

Regarding the constraints, (4b) models the demand fulfillment and captures the unsatisfied demand. Constraints (4c) and (4d) represent the number of evacuees at the SPs and DPs, respectively. Additionally, constraints (4e) and (4f) present the capacity constraints of SPs concerning the number of evacuees and relief items, respectively.

We next describe the constraints related to the inventory flow balance of relief items at an SP. Constraint (4h) is the inventory balance constraint for relief items at the SPs. The terms in (4h) are organized in a specific order to ensure an adequate supply of relief items to meet demand while satisfying the capacity constraints following the sequence of operation at SP $j \in J$, which is illustrated in Figure 1. First, the initial inventory $\ell_{j,0}$ and the emergency shipments at time t are available to fulfill demand. The remaining inventory after addressing demand becomes accessible for shipment to other SPs denoted as $j' \in J \setminus \{j\}$. Afterwards, the relief items dispatched from the MDC and all other SPs $j' \in J \setminus \{j\}$ are integrated into the inventory. Subsequently, any surplus items are shipped out to either mitigate inventory costs or comply with inventory storage constraints. Constraint (4g)

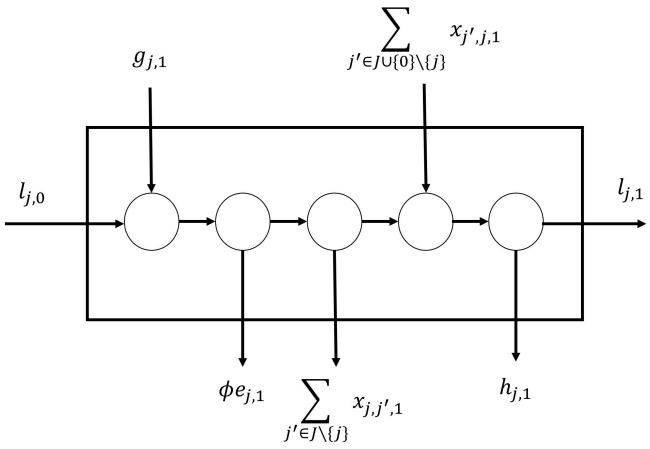

FIGURE 1 Sequence of flow of relief items at SP $j \in J$.

imposes the capacity constraints on the SPs. Additionally, constraint (4i) ensures that the total shipment among SPs does not surpass the available inventory.

3.1.2 | The stage–t problem

Recall that we made the assumption that the SP opening decisions are made only in the first stage. We thus use notation $\hat{z}_j,\ \forall j \in J$ to represent these decisions, which will be treated as input parameters to the stage-t problem at $t > 1$. The stage-t problem is similar to the first-stage problem, and the initial conditions are given by $\hat{X}_{t-1}$, the values of the state variables from $t-1$, including: $\hat{\ell}_{j,t-1},\ \forall j \in J$, $\hat{e}_{i,t-1},\ \forall i \in I$, and $\hat{e}_{j,t-1},\ \forall j \in J$. Given a realization of the Markovian state ξ_t, the initial condition $\hat{X}_{t-1}$, and first-stage SP activation decisions $\hat{z}$, we define the corresponding CTG function for the stage-t problem as follows:

$$Q_t(\hat{X}_{t-1}, \hat{z}, \xi_t) = \min \sum_{j \in J} (c^P + c^R_{0,j}) x_{0,j,t} + \sum_{j' \in J} \sum_{j \in J} c^R_{j',j} x_{j',j,t} + \sum_{i \in I} \sum_{j \in J} c^E_{i,j} y_{i,j,t} + \sum_{j \in J} c^G_j g_{j,t} +$$
$$\sum_{j \in J} c^H_j h_{j,t} + \sum_{i \in I} c^{PE}_i u_{i,t} + \sum_{j \in J} c^{InvE}_j e_{j,t} + \sum_{j \in J} c^{InvR}_j \ell_{j,t} + \mathcal{Q}^{\xi_t}_{t+1}(X_t, \hat{z}) \tag{5a}$$

$$\text{s.t.} \sum_{j \in J} y_{i,j,t} + u_{i,t} = D_{i,\xi_t} \hat{e}_{i,t-1},\ \forall i \in I \tag{5b}$$

$$\hat{e}_{i,t-1} - \sum_{j \in J} y_{i,j,t} = e_{i,t},\ \forall i \in I \tag{5c}$$

$$\hat{e}_{j,t-1} + \sum_{i \in I} y_{i,j,t} = e_{j,t},\ \forall j \in J \tag{5d}$$

$$e_{j,t} \le q_j \hat{z}_j,\ \forall j \in J \tag{5e}$$

$$\ell_{j,t} \le \phi q_j \hat{z}_j,\ \forall j \in J \tag{5f}$$

$$\hat{\ell}_{j,t-1} + g_{j,t} - \phi e_{j,t} \le \phi q_j \hat{z}_j,\ \forall j \in J \tag{5g}$$

$$\sum_{j' \in J, j \ne j'} x_{j,j',t} \le \hat{\ell}_{j,t-1} + g_{j,t} - \phi e_{j,t},\ \forall j \in J \tag{5h}$$

$$\hat{\ell}_{j,t-1} + x_{0,j,t} + \sum_{j' \in J, j' \ne j} x_{j',j,t} - \sum_{j' \in J, j \ne j'} x_{j,j',t} - \phi e_{j,t} + g_{j,t} - h_{j,t} = \ell_{j,t},\ \forall j \in J \tag{5i}$$

$$u_{i,t}, e_{i,t} \ge 0,\ \forall i \in I; e_{j,t}, \ell_{j,t}, h_{j,t}, g_{j,t} \ge 0,\ \forall j \in J \tag{5j}$$

$$y_{i,j,t} \ge 0,\ \forall i \in I,\ \forall j \in J; x_{j,j',t} \ge 0,\ \forall j \in J \cup \{0\},\ \forall j' \in J : j \ne j' \tag{5k}$$

In formulation (5), $\mathcal{Q}_{t+1}^{\xi_t}(X_t, \hat{z})$ is the expected CTG function at $t+1$ associated with Markovian state ξ_t, which is defined as:

$$\begin{aligned}\mathcal{Q}_{t+1}^{\xi_t}(X_t, \hat{z}) &= \mathbb{E}_{\xi_{t+1}|\xi_t}\left[Q_{t+1}(X_t, \hat{z}, \xi_{t+1})\right] \\ &= \begin{cases} \sum_{\xi_{t+1}\in\Xi_{t+1}} p_{\xi_t,\xi_{t+1}} Q_{t+1}(X_t, \hat{z}, \xi_{t+1}) & \text{if } \xi_t \text{ is } \textit{transient} \\ 0 & \text{if } \xi_t \text{ is } \textit{absorbing} \end{cases}\end{aligned} \tag{6}$$

3.2 | Alternative stochastic programming models and solution approaches

MSSP models are known to be computationally challenging to solve. We next discuss two alternative solutions approaches to MSSP that are based on a two-stage stochastic programming (2SSP) model.

3.2.1 | A two-stage stochastic programming model

The 2SSP model proposed here can be thought of as a restriction of the MSSP model in the sense that the decision sequence is reduced into two stages. Specifically, the decision associated with a set of state variables over all periods in the planning horizon, including the first-stage SP activation decisions, are made in the first stage. The stochastic evolution of hurricane, and thus the demand realization, is represented by a number of scenarios $\xi_s := (\xi_{1,s}, \cdots, \xi_{t_s,s})$, $\forall s \in S$, which, for example, can be generated by sampling from the underlying MC process. Here $t_s \leq T$ represents the period when the hurricane gets into an absorbing state under scenario s, which means that every scenario corresponds to a sequence of transient states followed by an absorbing state at the end. An optimal decision policy of a 2SSP model consists of the values of the first-stage decision variables and the values of the recourse decisions for each scenario $s \in S$.

3.2.2 | 2SSP as a stochastic look-ahead model

At any period $t \in \mathcal{T}$, one can define a 2SSP model according to the realized Markovian state ξ_t at t and a set of scenarios generated from ξ_t for the remainder of the planning horizon, which is referred to as a stochastic look-ahead model (SLAM) [37]. If the SLAM is only created and solved at $t = 1$, the corresponding decisions associated with the state variables over all the periods in the planning horizon are used in a static fashion regardless of the realization of uncertainty, which we refer to as the *static* 2SSP approach. The decision policy associated with static 2SSP entirely loses the adaptability of the state variables according to the realization of uncertainty, as the same values for the first-stage state variables are applied to all hurricane scenarios. This motivates the so-called rolling-horizon procedure that applies the 2SSP model at each period t as a SLAM for the remainder of the planning horizon, where only the decisions associated with the current period t are implemented. In this case, the adaptability of the decision policy directly comes from the newly realized information used to construct the SLAM in each period t. For generality, we next present the 2SSP model that is used as a SLAM starting at any period $t' < T$ for the IHERLP problem.

We consider a 2SSP model used as a SLAM starting at any period $t' < T$ with the planning horizon defined as $\{t', t'+1, \ldots, T\}$. The first-stage variables include $\ell_{j,t}$, $\forall j \in J, \forall t \in \{t', t'+1, \ldots, T\}$, which correspond to the inventory levels at SPs for the entire planning horizon. We emphasize that, variables $e_{j,t}$, $\forall j \in J$ and $e_{i,t}$, $\forall i \in I$, for all $t \in \{t'+1, \cdots, T\}$, which are defined as state variables in the MSSP model (4) and (5), are not treated as the state variables in 2SSP model. This is because contrary to the inventory of relief items $\ell_{j,t}$ at SP j, which are treated as the state variables since the corresponding recourse decisions to transport relief items in or out from the SPs are readily available in the form of $g_{j,t}$ and $h_{j,t}$, this simple recourse cannot be applied to the number of evacuees at SPs $e_{j,t}$ and DPs $e_{i,t}$ since we cannot force people to evacuate if the evacuation demand is lower than expected. In other words, treating $e_{j,t}$ and $e_{i,t}$ variables as state variables is inappropriate from a practical perspective in our 2SSP model. Instead, these decisions are defined as the second-stage decisions, dependent on the demand realization associated with each sample path. This marks a major difference between our MSSP and 2SSP models. The 2SSP model has only the state variables on the logistics side of the network and requires the complete sample path information $\xi_{t',s}, \cdots, \xi_{t_s,s}$ for the recourse decisions for each sample path s.

The SP activation decisions $\{z_j\}_{j\in J}$ are also the first-stage variables in the SLAM defined at $t' = 1$, but their values will be used as input parameters for the SLAM defined for any $t' > 1$, according to Assumption 2. All the local variables defined in

model (4) and (5) associated with period t' are naturally also the first-stage decisions, and all other local variables, i.e., those defined for $t \in \{t'+1, \cdots, T\}$, are defined as second-stage decision variables. We next describe in detail the first-stage and second-stage problems associated with the 2SSP model defined at period $t' < T$. We note that unlike the MSSP model, terms "stage" and "period" cannot be used interchangeably to describe the 2SSP model.

3.2.3 | The first-stage problem of SLAM at $t' = 1$

When $t' = 1$, the input parameters correspond to the same initial conditions as the first-stage problem of the MSSP model (4a). The key distinction of the first-stage problem of SLAM at $t' = 1$ from $t' > 1$ is the incorporation of the SPs activation decisions at $t' = 1$ with the corresponding fixed costs accrued on the process which is presented as follows:

$$\begin{aligned}\min\ & \sum_{j\in J}(c_j^F + c_j^f \times |T|)z_j + \sum_{j\in J}(c^P + c_{0,j}^R)x_{0,j,1} + \sum_{j\in J}\sum_{j'\in J\setminus\{j\}} c_{j,j'}^R x_{j,j',1} + \sum_{i\in I}\sum_{j\in J} c_{i,j}^E y_{i,j,1} \\ & + \sum_{j\in J} c_j^G g_{j,1} + \sum_{j\in J} c_j^H h_{j,1} + \sum_{i\in I} c_i^{PE} u_{i,1} + \sum_{j\in J} c_j^{InvE} e_{j,1} + \sum_{t\in\{1,\cdots,T\}}\sum_{j\in J} c_j^{InvR}\ell_{j,t} + \sum_{s\in S} p_s\theta_s \qquad (7a)\\ \text{s.t. } & \text{(4b) – (4e) and (4g) – (4i)} \\ & \ell_{j,t} \le \phi q_j z_j,\ \forall j \in J,\ \forall t \in \{1,2,\cdots,T\}, \qquad (7b)\end{aligned}$$

where θ_s is introduced to represent the second-stage objective value for each scenario $s \in S$ in a Benders decomposition framework, as will be explained in more detail in Section 4.

3.2.4 | The first-stage problem of SLAM at $t' > 1$

When $t' > 1$, the input parameters to the 2SSP model defined over the planning horizon of $\{t', t'+1, \ldots, T\}$ include: (i) the values of the state variables from $t'-1$, including $\{\hat{\ell}_{j,t'-1}\}_{j\in J}$; (ii) the number of evacuees at SPs and DPs at $t'-1$, i.e., $\{\hat{e}_{j,t'-1}\}_{j\in J}$ and $\{\hat{e}_{i,t'-1}\}_{i\in I}$, respectively; and (iii) the realization of the Markovian state $\xi_{t'}$ at t'. The solution to z variables $\{\hat{z}_j\}_{j\in J}$ from the problem (7) at $t' = 1$ is used as an input parameter. The resulting first-stage model is as follows:

$$\begin{aligned}\min\ & \sum_{j\in J}(c^P + c_{0,j}^R)x_{0,j,t'} + \sum_{j\in J}\sum_{j'\in J\setminus\{j\}} c_{j,j'}^R x_{j,j',t'} + \sum_{i\in I}\sum_{j\in J} c_{i,j}^E y_{i,j,t'} + \\ & \sum_{j\in J} c_j^G g_{j,t'} + \sum_{j\in J} c_j^H h_{j,t'} + \sum_{i\in I} c_{t'}^{PE} u_{i,t'} + \sum_{j\in J} c_j^{InvE} e_{j,t'} + \sum_{t\in\{t',\cdots,T\}}\sum_{j\in J} c_j^{InvR}\ell_{j,t} + \sum_{s\in S} p_s\theta_s \qquad (8a)\\ \text{s.t. } & \text{(4b) – (4d) and (4h) – (4i) applicable at } t' \\ & \text{(4e) and (4g) applicable at } t' \text{ with variables } \{z_j\}_{j\in J} \text{ replaced by } \{\hat{z}_j\}_{j\in J} \\ & \ell_{j,t} \le \phi q_j \hat{z}_j,\ \forall j \in J,\ \forall t \in \{t', \cdots, T\} \qquad (8b)\end{aligned}$$

3.2.5 | The second-stage problem of the 2SSP model

For the 2SSP model defined as a SLAM over the planning horizon of $\{t', t'+1, \ldots, T\}$, the second-stage variables include all the local decision variables as well as $\{e_{i,t}\}_{i\in I}$ and $\{e_{j,t}\}_{j\in J}$ at $t \in \{t'+1, t'+2, \ldots, T\}$. A set of scenarios S is given, where each scenario $s \in S$ represents a sample path of the hurricane's evolution from $t'+1$ until the respective landfall period $t_s \le T$, which occurs with probability p_s. The corresponding demand realization vector under a sample path $s \in S$ is represented as $(\{D_{i,t'+1,s}\}_{i\in I}, \{D_{i,t'+2,s}\}_{i\in I}, \ldots, \{D_{i,t_s,s}\}_{i\in I})$. The second-stage problem of the 2SSP model defined over the planning horizon of $\{t', t'+1, \ldots, T\}$ is defined as follows:

$$\begin{aligned}\min\ & \sum_{t\in\{t'+1,\ldots,T\}}\Bigg(\sum_{i\in I}\sum_{j\in J} c_{i,j}^E y_{i,j,t,s} + \sum_{j\in J} c_j^{InvE} e_{j,t,s} + \sum_{j\in J}(c^P + c_{0,j}^R)x_{0,j,t,s} + \sum_{j\in J}\sum_{j'\in J} c_{j,j'}^R x_{j,j',t,s} + \\ & \sum_{j\in J} c_j^G g_{j,t,s} + \sum_{j\in J} c_j^H h_{j,t,s} + \sum_{i\in I} c_i^{PE} u_{i,t,s}\Bigg) - \Bigg(\sum_{t\in\{t_s+1,\ldots,T\}}\sum_{j\in J} c_j^{InvR}\ell_{j,t}\Bigg)\cdot \mathbb{I}_{[t_s<T]} \qquad (9a)\end{aligned}$$

$$\text{s.t.} \sum_{j\in J} y_{i,j,t,s} + u_{i,t,s} = D_{i,t,s}e_{i,t-1,s},\ \forall i \in I, \forall t \in \{t'+1, ..., t_s\} \tag{9b}$$

$$e_{i,t,s} = e_{i,t-1,s} - \sum_{j\in J} y_{i,j,t,s},\ \forall i \in I, \forall t \in \{t'+1, ..., t_s\} \tag{9c}$$

$$e_{i,t',s} = \hat{e}_{i,t'},\ \forall i \in I \tag{9d}$$

$$e_{j,t,s} = e_{j,t-1,s} + \sum_{i\in I} y_{i,j,t,s},\ \forall j \in J, \forall t \in \{t'+1, ..., t_s\} \tag{9e}$$

$$e_{j,t',s} = \hat{e}_{j,t'},\ \forall j \in J \tag{9f}$$

$$e_{j,t,s} \le q_j\hat{z}_j,\ \forall j \in J, \forall t \in \{t'+1, ..., t_s\} \tag{9g}$$

$$\hat{\ell}_{j,t-1} + x_{0,j,t,s} + \sum_{j'\in J, j\neq j'} x_{j',j,t,s} - \sum_{j'\in J, j\neq j'} x_{j,j',t,s} - \phi e_{j,t,s} + g_{j,t,s} - h_{j,t,s} = \hat{\ell}_{j,t},$$
$$\forall j \in J, \forall t \in \{t'+1, ..., t_s\} \tag{9h}$$

$$\sum_{j'\in J, j\neq j'} x_{j,j',t,s} \le \hat{\ell}_{j,t-1} + g_{j,t,s} - \phi e_{j,t,s},\ \forall j \in J, \forall t \in \{t'+1, ..., t_s\} \tag{9i}$$

$$\hat{\ell}_{j,t-1} + g_{j,t,s} - \phi e_{j,t,s} \le \phi q_j\hat{z}_j,\ \forall t \in \{t'+1, ..., t_s\}, \forall j \in J \tag{9j}$$

$$u_{i,t,s}, e_{i,t,s} \ge 0,\ \forall i \in I, \forall t \in \{t'+1, \cdots, t_s\} \tag{9k}$$

$$y_{i,j,t,s} \ge 0,\ \forall i \in I,\ \forall j \in J, \forall t \in \{t'+1, \cdots, t_s\} \tag{9l}$$

$$x_{j,j',t,s} \ge 0,\ \forall j \in J \cup \{0\},\ \forall j' \in J : j \neq j', \forall t \in \{t'+1, \cdots, t_s\} \tag{9m}$$

$$e_{j,t,s}, g_{j,t,s}, g_{j,t,s} \ge 0,\ \forall j \in J, \forall t \in \{t'+1, \cdots, t_s\}. \tag{9n}$$

We note that the second component of the objective function (9a) models the "reimbursement" [45] of the first-stage logistics costs incurred after the terminating stage t_s for scenario $s \in S$ if $t_s < T$. After solving the first-stage problem, we obtain the values for the inventory decisions $\hat{\ell}_{j,t},\ \forall t = t', \cdots, T$. But since under a particular scenario $s \in S$ with terminal period $t_s < T$, the first-stage inventory decisions $\hat{\ell}_{j,t},\ \forall t \in \{t_s+1, \cdots, T\}$ are not implemented. The second component of the objective function (9a) is thereby introduced to represent the return on the *planned but unused* inventory after hurricane's termination in scenario s. In terms of the constraints, (9d) and (9f) are used to make scenario copies of the first-stage decisions for the number of evacuees, which ensure that the number of evacuees at DPs and SPs at t' are the same under all scenarios.

4 | SOLUTION METHODS FOR THE 2SSP AND MSSP MODELS

We apply the stochastic dual dynamic programming (SDDP) and Benders decomposition (BD) algorithms to solve the MSSP and 2SSP models, respectively [19, 27]. Since these algorithms are standard approaches in the literature to solve the respective stochastic programming models, we briefly describe the general approach and present the derivations of the cutting planes used in our setting.

4.1 | Benders decomposition for 2SSP

To implement BD for solving the 2SSP model, we decompose the 2SSP problem into two problems: a master problem (MP) and a set of subproblems, one for each scenario. The initial MP is a relaxation of the first-stage 2SSP model (7) in which a continuous non-negative variable θ_s substitutes the second-stage problem for each scenario $s \in S$, representing the second-stage value. The second-stage model (9) is decomposed into $|S|$ subproblems, one for each $s \in S$. The vanilla version of the BD algorithm can be described as follows. Since MP is a relaxed problem, its optimal solution provides a lower bound (LB) of the original problem. The MP is solved to achieve relaxed first-stage solutions. The subproblem for each $s \in S$ is feasible for any feasible MP solution in our problem because of the relatively complete recourse. Once MP is solved optimally, the subproblem is solved for each scenario $s \in S$ by replacing the first-stage variables in the problem with the optimal MP solutions. The overall objective value for the optimal first-stage solutions from MP and the optimal second-stage solutions from the subproblems becomes an upper bound (UB) of the original problem.

We reformulate all the constraints in the subproblems by moving the given first-stage solutions to the right-hand side (RHS) of the second-stage constraints. We rewrite the inequality constraints as the "$\geq$" constraints for standardization. Given a first-stage solution $(\hat{e}, \hat{\ell}, \hat{z}, \hat{\theta})$, let $\lambda^{(9d)}_{i,t',s}$, $\lambda^{(9f)}_{j,t',s}$, $\lambda^{(9g)}_{j,t,s}$, $\lambda^{(9h)}_{j,t,s}$, $\lambda^{(9i)}_{j,t,s}$, and $\lambda^{(9j)}_{j,t,s}$ be the optimal dual solutions associated with the constraints (9d), (9f), (9g), (9h), (9i), (9j), and (9k), respectively. We generate and add the Benders optimality cut (10) to the MP at $t' = 1$ if it is violated by the first-stage solution $(\hat{e}, \hat{\ell}, \hat{z}, \hat{\theta})$, for each scenario $s \in S$. For the MP at $t' > 1$, since the solution of z variables obtained from solving the SLAM at $t' = 1$ are used in the formulation (8), Benders cut (11) is generated, where the terms associated with solution $\hat{z}$ appear as constants, and added to the MP if it is violated by the first-stage solution $(\hat{e}, \hat{\ell}, \hat{\theta})$, for each scenario $s \in S$.

Benders cut for MP at $t' = 1$

$$\theta_s \geq \sum_{i\in I} \lambda^{(9d)}_{i,t',s} e_{i,t'} + \sum_{j\in J} \lambda^{(9f)}_{j,t',s} e_{j,t'} + \sum_{j\in J} \sum_{t\in\{t'+1,\ldots,t_s\}} \left(-\lambda^{(9g)}_{j,t,s} q_j z_j + \lambda^{(9h)}_{j,t,s} \ell_{j,t} + \left(-\lambda^{(9h)}_{j,t,s} - \lambda^{(9i)}_{j,t,s} + \lambda^{(9j)}_{j,t,s}\right) \ell_{j,t-1} - \lambda^{(9j)}_{j,t,s} \phi q_j z_j\right) \tag{10}$$

Benders cut for MP at $t' > 1$

$$\theta_s \geq \sum_{j\in J} \sum_{t\in\{t'+1,\ldots,t_s\}} \left(-\lambda^{(9g)}_{j,t,s} q_j \hat{z}_j - \lambda^{(9j)}_{j,t,s} \phi q_j \hat{z}_j\right) + \sum_{i\in I} \lambda^{(9d)}_{i,t',s} e_{i,t'} + \sum_{j\in J} \lambda^{(9f)}_{j,t',s} e_{j,t'} + \sum_{j\in J} \sum_{t\in\{t'+1,\ldots,t_s\}} \left(\lambda^{(9h)}_{j,t,s} \ell_{j,t} + \left(-\lambda^{(9h)}_{j,t,s} - \lambda^{(9i)}_{j,t,s} + \lambda^{(9j)}_{j,t,s}\right) \ell_{j,t-1}\right) \tag{11}$$

The cuts are added to the MP iteratively until the desired gap between *LB* and *UB* is achieved. The BD algorithm can be integrated in the branch-and-bound procedure for solving the MP via the lazy constraint callback in modern integer programming solvers such as Gurobi.

4.2 | Stochastic dual dynamic programming for MSSP

We apply the SDDP algorithm to solve the MSSP model defined in (4) and (5). In SDDP, the expected CTG functions $\mathcal{Q}^{\xi_t}_{t+1}(\cdot)$, defined via the dynamic programming equations (4) and (5), are approximated by a convex piecewise linear under-estimator. By a sequence of forward and backward passes applied on the randomly drawn samples from the scenario tree (with respect to the underlying MC process), the under-approximation functions are updated by adding the Benders optimality cuts. To do so, we adopt a standard epigraph representation and introduce variables θ^{ξ_t} for each Markovian state $\xi_t \in \Xi_t$ to represent the corresponding expected CTG function. One subtlety here is that since the SP opening decisions z_j are made at the first stage, we introduce auxiliary variables, $z_{j,t}$ to make a copy of all z_j variables locally for each expected CTG function for $t > 1$ as follows:

$$z_{j,t} = \hat{z}_j, \ \forall j \in J \tag{12}$$

We note that it is important that local copies of these first-stage integer solutions z, applicable across all periods, are employed. This allows for the propagation of complete first-stage solution information to subsequent CTG functions, which ensures that cuts are introduced at the first stage with respect to all z variables. Given that the local variables $z_{j,t}$ in (12) encapsulate the solution $\hat{z}_j$ pertinent to the CTG functions $Q_t(\cdot)$, we replace $\hat{z}_j$ in constraints (5e), (5f), and (5g) by the local variable $z_{j,t}$. This substitution ensures the consistency in the representation of the first-stage solution information across all periods.

Illustration of the SDDP algorithm

The SDDP algorithm unfolds as an iterative process. In each iteration k of SDDP, we solve the first-stage problem, incorporating the Benders cutting planes introduced up to iteration $k-1$ to approximate the second-stage expected CTG function $\mathcal{Q}^{\xi_1}_2(\cdot)$, and obtain a first-stage solution $\hat{X}_1$. Subsequently, we draw a Monte-Carlo sample and obtain a sample path s: $(\hat{\xi}_{2,s}, \hat{\xi}_{3,s}, \cdots, \hat{\xi}_{t_s,s})$ based on transition probabilities of the underlying MC model, where t_s is the terminal stage of sample path s, meaning that state $\hat{\xi}_{t_s,s}$ is an absorbing state.

Given the first-stage solution $\hat{X}_1$ and the Markovian state $\hat{\xi}_{2,s}$ sampled at $t = 2$, we solve the corresponding stage-2 problem with the current approximation of the associated expected CTG function $\mathcal{Q}^{\hat{\xi}_{2,s}}_3(\cdot)$ and obtain $\hat{X}_2$. The sequential resolution of all stage-t problems follows, employing solutions $\hat{X}_{t-1}$ and the realized hurricane Markovian states $\hat{\xi}_{t,s}$ for $t = 3, 4, \cdots, t_s$. This

sequential process is referred to as the forward pass of the SDDP algorithm. An example of the forward pass on a random sample is presented in Figure A2 in the Appendix.

Following the sample path obtained from the forward pass and the solutions obtained along the sample path, $\hat{X}_1, \hat{X}_2, \cdots, \hat{X}_{t_s}$, we start the backward pass. During this pass, we go back in time, i.e., from $t = t_s, t_s - 1, \cdots, 1$, and generate Benders optimality cuts with $\hat{X}_t$ chosen as the reference points and incorporate them into the respective stage-t problems in each stage t. These cuts will be used to improve the approximations to the expected CTG functions. We note that no cuts are generated for the expected CTG function corresponding to any absorbing state. An illustration of this process is presented in Figure A3 in the Appendix. It is important to note that not all the Markovian states in stage t are accessible from the states in stage $t-1$ based on the transition probabilities of the MC. However, we solve all the stage-t problems associated with all the Markovian states $\xi_t \in \Xi_t$ using solutions $\hat{X}_t$'s collected from the forward pass for the purpose of cut sharing. The cut sharing idea is applicable to the IHRLEP problem given the relatively complete recourse property, i.e., solution $\hat{X}_t$ is always feasible given any $\hat{X}_{t-1}$ in all possible states ξ_t. An illustration of cut sharing is presented in Figure A4 in the Appendix. After solving all stage-t problems for all states ξ_t, we generate cut coefficients using optimal dual solutions and introduce the aggregated cuts (weighted by the transition probabilities) to all the expected CTG function approximation associated with ξ_{t-1}.

Specifically, let $\alpha^{\xi_t}_{(5b)}, \cdots, \alpha^{\xi_t}_{(5g)}$ be the dual solutions associated with constraints (5b), $\cdots$,(5g) and let $\alpha^{\xi_t}_{(12)}$ be the dual solutions associated with constraint (12), that are used to approximate the expected CTG function associated with Markovian state ξ_t. At an iteration L of the algorithm, let $a^{\xi_t}_l$ be the constant of cuts added at iterations $l = 1, \cdots, L-1$ to the CTG function of state ξ_t and $\beta^{\xi_t}_l$ be the dual coefficients associated with the cuts. The under-approximation of the expected CTG function $\mathcal{Q}^{\xi_t}_{t+1}(\cdot)$ is updated at every iteration by adding the cut as follows:

$$\begin{aligned}\theta^{\xi_t} \geq \sum_{\xi_{t+1}\in\Xi_{t+1}} q_{\xi_t,\xi_{t+1}} \Bigg[& \sum_{i\in I} \left(\left(D_{i,\xi_{t+1}} \alpha^{\xi_{t+1}}_{(5b),i} + \alpha^{\xi_{t+1}}_{(5c),i} \right) e_{i,t} \right) \\ & + \sum_{j\in J} \left(\alpha^{\xi_{t+1}}_{(5d),j} e_{j,t} + \left(-\alpha^{\xi_{t+1}}_{(5i),j} - \alpha^{\xi_{t+1}}_{(5h),j} + \alpha^{\xi_{t+1}}_{(5g),j} \right) \ell_{j,t} \right) \\ & + \sum_{t'\in T} \sum_{j\in J} \alpha^{\xi_{t+1}}_{(12),j,t'} z_{j,t'} + \sum_{l=1}^{L} \beta^{\xi_{t+1}}_l a^{\xi_{t+1}}_l \Bigg] \end{aligned} \tag{13}$$

In each iteration of SDDP, the under-approximation of the expected CTG functions $\mathcal{Q}^{\xi_t}_{t+1}(\cdot)$ are updated for all Markovian states ξ_t for all $t \in \mathcal{T}$ via cut sharing. Throughout the SDDP algorithm, the LB is updated as the optimal objective value of the first-stage problem in each iteration. Following any iteration, a statistical UB can be computed by collecting the cumulative objective values over a number of randomly generated sample paths. Let $\bar{\mu}$ and $\bar{\sigma}$ be the sample mean and sample standard deviation of the total cost on the forward pass, respectively, of M randomly generated samples. We compute the statistical UB (confidence interval) with 95% confidence as:

$$UB = \bar{\mu} \pm 1.96 \times \frac{\bar{\sigma}}{\sqrt{M}}$$

The SDDP algorithm is shown to converge with probability one [36]. One could create a stopping criterion based on the gap between LB and the statistical UB. We choose to implement a practical termination criterion that keeps track of the LB progress: we terminate the SDDP procedure if the LB fails to improve beyond a specified threshold over a user-defined number of iterations.

5 | EXPERIMENTAL SETUP

In this section, we discuss our experiment setup and the computational results. We present case studies motivated by Hurricane Florence 2018 and Hurricane Ian 2022 with the assumption of deterministic and random landfall time, respectively. We start by discussing how we model the forecast uncertainty for the purpose of scenario generation.

5.1 | Modeling forecast errors

The way we model hurricane forecast errors depends on the assumption on whether the terminal period is deterministic or random for the proposed MSSP and 2SSP models, depending on whether the landfall time is assumed to be deterministic or

random. For the deterministic landfall time case, we use the NHC's historical track and intensity forecast error (FE) data to generate scenarios, whereas for the random landfall case, we use NHC's *along*, *cross*, and intensity FE data. Our stochastic model for characterizing the FE is constructed based on data available from the NHC's forecast verification report [5], which is released each year at the end of every hurricane season. The forecast verification is done by comparing the point forecast made at a period, for all periods up to five days in the future, against the the actual hurricane trajectory commonly known as *best track*. At any time of the historical point forecast, the forecast errors are available for the forecast made for 12, 24, 36, 48, 72, 96, and 120 hours in the future. However, as stated by Assumption 3, our model requires each period to be 12 hours long. Hence we introduce forecast errors at 60 and 108 hours as the average of the errors at 48 and 72 hours, and 96 and 120 hours, respectively.

The track FE at each period is defined as the great circle distance, which gives an absolute distance between the forecast track and the best track. The along and cross errors are the actual trajectory FE along the direction and across the orthogonal direction of the point forecast. The intensity error is given as the difference between the forecast and the best track wind speed. An illustration of these concepts is presented in Figure A5 in the Appendix.

5.1.1 | A time-series model of the FE process from historical data

Our preliminary data analysis indicates that the Pearson correlation coefficient [16] of FE between two subsequent periods is greater than 0.5 for all types of FEs described above. The results are deferred to Figure A6 in the Appendix. We also observe that the Pearson correlation coefficient of FEs associated with two non-consecutive periods decreases as the number of periods in between increases. This motivates us to model the FE process using the autoregressive model of order one (AR-1) [12], which captures the Markovian structure of the FE process exhibited in the historical data.

Specifically, let η_t represent the FE at period t, then according to the AR-1 model, we have: $\eta_t = \rho\eta_{t-1} + \epsilon_t$, where $\epsilon_t \overset{\text{iid}}{\sim} N(0, \sigma^2)$, $\forall t \in \mathcal{T} \setminus \{1\}$ and η_1 is deterministic. It is clear that the AR-1 model assumes the FE data to be normally distributed at every period. We thereby perform a normality test with the support of box plots and quantile-quantile (Q-Q) plots [14] for intensity, along, and cross errors. An illustration of the FEs at 024 hours is presented in Figures A7 and A8 in the Appendix. In contrast, the great-circle track error is not normally distributed which is shown in Figures A9a and A9b in the Appendix. The non-normal distribution of the track FE is due to heavy tails observed. To address this, we transform the track FE data using a log transformation as follows:

$$\eta_t^{trans} = \log(\eta_t + 1), \ \forall t \in \mathcal{T} \setminus \{1\},$$

where η_t^{trans} is the transformed track FE, η_t is the original track FE, and 1 is added to avoid $\log(0)$ in absolute track FE data. We see that the normality assumption is valid after the transformation which is supported by Figures A9c and A9d in the Appendix.

5.1.1.1 | *Parameter estimation for the AR-1 model*

We estimate parameters (ρ, σ) in the AR-1 model using the maximum likelihood estimation (MLE) based on the NHC's official FE data of tropical storms from 2017 to 2021 [5], and we denote the estimated parameters as ρ_{mle} and σ^2_{mle}. At any period t, the FE $\eta_t = \rho_{mle}\eta_{t-1} + \epsilon_t$; $\epsilon_t \sim N(0, \sigma^2_{mle})$. The estimated parameters are presented in Table A1 in the Appendix. Given η_{t-1}, ρ_{mle} and σ^2_{mle}, a realization of η_t can be obtained by sampling $\epsilon_t \sim N(0, \sigma^2_{mle})$.

5.1.1.2 | *Independence between different types of FEs*

So far we have discussed the Markovian structure of individual FE processes (implied by the AR-1 models). Since the demand is a function of both hurricane track and intensity, we are interested in constructing hurricane scenarios with a joint distribution of the FEs. We use unidirectional track FEs with the point track forecast to create track scenarios in case of deterministic landfall case. In case of random landfall, we use along and cross FEs to create track scenarios. The Pearson correlation coefficients shown in Table A2 and the scatter plots shown in Figure A10 in the Appendix indicate that the intensity, track, along, and cross FEs are roughly independent to each other. The independence of FEs allows us to create hurricane scenarios by sampling each type of FE independently and then combine them together with their joint transition probabilities computed as the product of their individual transition probabilities.

5.2 | Instance generation for the Hurricane Florence case study

Hurricane Florence made landfall in the states of North Carolina and South Carolina in 2018. In this computational experiment, we present the IHRLEP problem for the State of South Carolina considering a deterministic landfall time. We consider a

planning horizon of five days (or equivalently, 120 hours) prior to the projected landfall time given by the NHC forecast. The total number of periods in the planning horizon is 11, each being 12 hours long, starting at 120 hours ($t = 0$) prior to landfall. We assume that the hurricane makes landfall deterministically at $t = 10$. We assume that the coastal line of South Carolina is straight for simplicity. We define the study region as an area extending 200 miles around the endpoints of the 170-mile-long coastal line.

5.2.1 | Demand and shelter points generation

Hurricanes that make landfall beyond the study region produce zero demand at all DPs. We assume the ZIP code locations of eight coastal SC counties that are within 50 miles from the coastal line are vulnerable to a hurricane landfall within the study region. We represent the DPs' locations by projecting the geographical locations of all vulnerable ZIP codes onto the coastal line. We set $\bar{D}_i$, $\forall i \in I$ to be 5% of the vulnerable population of the respective DPs [6]. Since the number of ZIP codes in a vulnerable region is too large to consider each of them as an independent DP, we use the K-Means clustering approach [26] to cluster the projected locations and population into $|I| = 10$, to represent the DPs to our model. Furthermore, the SC Emergency Management Division (SCEMD) maintains a list of candidate SPs in every county of SC. Similarly, we use K-Means clustering with $|J| = 10$ to generate the candidate SPs by the cluster centers for the location with the capacity aggregated. A visual representation of the shelters at the county level and an example of this aggregation is shown in Figure A12 in the Appendix. We pick the central location of Greenville county as the location of MDC and assume that it has an unlimited supply capacity of relief items. The logistics network of South Carolina for Florence case study is shown in Figure 2a.

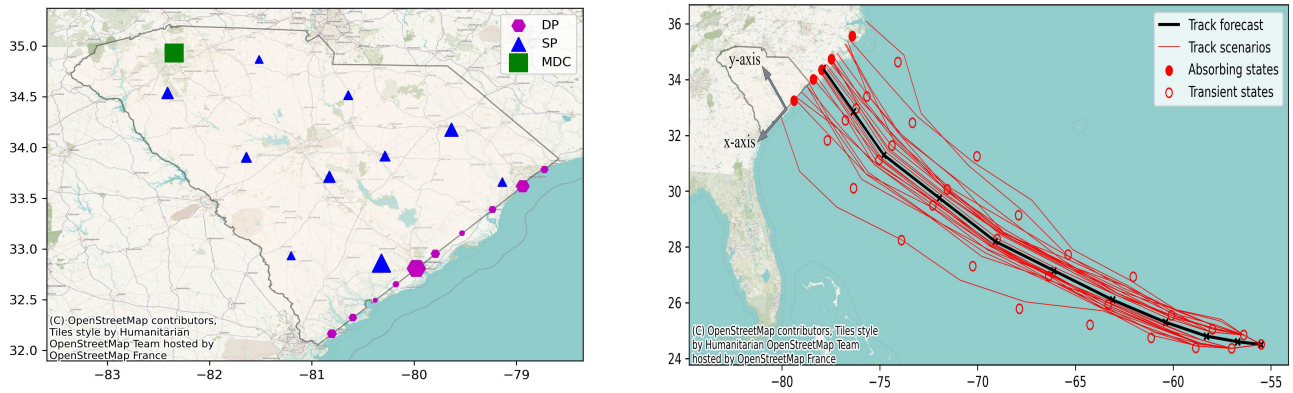

FIGURE 2 An illustration of locations (of DPs, SPs, and the MDC), hurricane scenarios, and MC discretization for Hurricane Florence case study. The sizes of the markers representing SPs/DPs are proportional to their capacity and demand levels, respectively.

5.2.2 | Hurricane scenario generation

A hurricane scenario ξ_t at time $t \in \mathcal{T}$ is defined by its location and intensity, denoted as: $\xi_t := (\xi_{t,x}, \xi_{t,y}, \xi_{t,int})$, where $\xi_{t,x,y} := (\xi_{t,x}, \xi_{t,y})$ represents the spatial coordinates and $\xi_{t,int}$ represents the intensity, measured as the hurricane category on the Saffir-Simpson scale. We use track and intensity AR-1 error models with Hurricane Florence's point forecast given by NHC 120 hours prior to its landfall to generate hurricane scenarios. Since the track error is a great-circle distance, we only have information about the magnitude of the error but not the direction. Hence, to come up with a case study with deterministic landfall time, we make the following assumptions about the evolution of Hurricane Florence: (i) the forward speed of the hurricane, i.e., the movement along the direction orthogonal to the study region (y–axis), is deterministic at each period and is given by NHC's point forecast; (ii) the movement of the hurricane along the direction parallel to study region (x–axis) is random which is given

by the point forecast and the track error sampled from AR-1 model for track error. The directions of the x- and y-axes are shown in Figure 2b.

Since the track errors are given in the absolute great circle distance, sampled track errors are either added to or subtracted from the point forecast along x–axis, for the entire path, which is decided based on a random Bernoulli trial, to create track scenarios. Since the AR-1 FE samples for track error are the *log*–transformed, we *restore* the transformation using the following rule:

$$\hat{\eta}_t \leftarrow e^{\hat{\eta}_t^{trans}} - 1, \ \forall t \in \mathcal{T} \setminus \{1\},$$

where $\hat{\eta}_t^{trans}$ is the sampled track error from the AR-1 model of the log–transformed track FE, and $\hat{\eta}_t$ is the original track FE error after restoring the transformation. Since the AR-1 model for the transformed track FE has a low variance and we assume $\eta_1 = 0$, we observe a very low variability in track FE samples which does not sufficiently represent the true distribution. Hence for the sake of sufficient variability in the track samples, we fix the absolute track FE at $t = 2$ to be the average absolute track error from historical data. In sampling, the same random Bernoulli trial is applied at $t = 2$ to create scenarios at either sides of the forecast. An example of the track scenarios is shown in Figure 2b. In the figure, the transient and absorbing states depict the discretized Markovian states for MSSP, which we will elaborate in Section 5.4. The intensity scenarios are created by adding the intensity error samples to the intensity point forecast. The resulting intensity in terms of wind speed is represented by the respective hurricane categories indicated by Saffir-Simpson (SS) hurricane wind scale.

5.2.3 | Demand estimation

In addition to hurricane position and intensity, SCEMD estimates the demand based on additional factors such as storm surge and flood warnings. In fact, demand estimation/prediction for hurricane evacuation is itself a complex problem that has been extensively studied in the literature, see, e.g., [38]. For simplicity, we estimate demand based on the distance of DPs from the hurricane position, hurricane intensity, and the lead time (τ) which is the number of periods until the hurricane's landfall. While the distance and intensity are random, the lead-time is deterministic in this case study as we assume a deterministic landfall time. Since we assume a deterministic forward speed, and the deviation of the hurricane track occurs only along the x–axis, we use the distance of the hurricane's position from the DPs along x– and y– axes as the basis of demand realization according to location, and lead-time, respectively. In practice, evacuation is completed in 2 – 3 days prior of hurricane landfall [28]. Hence we assume that the evacuation operation begins at $t = 4$, i.e., six periods before the landfall. We set $y_{\max}$ as the distance of the hurricane's location at $t = 4$ given by the point forecast and the hurricane's landfall location, so that demand at $t < 4$ is zero at all DPs. We define $x_{\max}$ as the extent, measured in miles, of the study region, representing the length of the coastal area extended by 200 miles from each endpoint in a straight line, that is, $x_{\max} = 2 \times 200 + 170 = 570$.

A positive demand (D_{i,ξ_t}) for DP $i \in I$ at a period t, as a product of demand realization according to intensity(D^{int}_{i,ξ_t}), lead time(D^{τ}_{i,ξ_t}), and location(D^{loc}_{i,ξ_t}), will incur if its location, given by its x- and y-coordinates: $L_{i,x}$ and $L_{i,y}$, respectively, is within a certain threshold in both the x- and y- axes, $x_{\max}$ and $y_{\max}$, respectively, which is given by:

$$\begin{aligned} D_{i,\xi_t} :=& D^{\text{int}}_{i,\xi_t} \times D^{\tau}_{i,\xi_t} \times D^{\text{loc}}_{i,\xi_t} \\ =& \frac{\xi_{t,int}}{int_{\max}} \times \left(1 - \frac{|\xi_{t,x} - L_{i,x}|}{x_{\max}}\right) \times \left(1 - \frac{|\xi_{t,y} - L_{i,y}|}{y_{\max}}\right) \end{aligned} \tag{14}$$

5.3 | Instance generation for the Hurricane Ian case study

Hurricane Ian 2022 made landfall in Florida [3]. Contrary to the Hurricane Florence case for the state of SC, an irregular geographical shape of the coastline of Florida imposes challenges if one restricts to the deterministic landfall time setting. In the random landfall time case, the hurricane track error scenarios are created using both the along and cross FEs of the hurricane track. In this case, we categorize the hurricane states as either transient or absorbing based on the actual coordinates of the hurricane's location and its relative distance to the study region of the state of Florida. The landfall time corresponds to the first period that the hurricane reaches an absorbing state. For this case study we consider a planning horizon of $T = 16$ periods. Since the point forecast by NHC is only available up to 11 periods, we use the moving average of two forecast points as the point forecast for $t > 11$. We proceed by defining the logistics network of this case study.

5.3.1 | Demand and shelter point generation

The Florida Division of Emergency Management categorizes the state of Florida into ten hurricane regions [4]. Each region has a set of available shelters at different locations and an estimated number of vulnerable people who would evacuate to public shelters. We represent each hurricane region as one candidate SP with their capacities aggregated at the central location of the region. We consider ten DPs, one for each hurricane region, with the aggregated demand located at the nearest GIS location at the coastline. The location of the MDC is picked randomly, away from the coastline, at the location with high population assuming sufficient availability of the relief items. All locations are illustrated in Figure 3a.

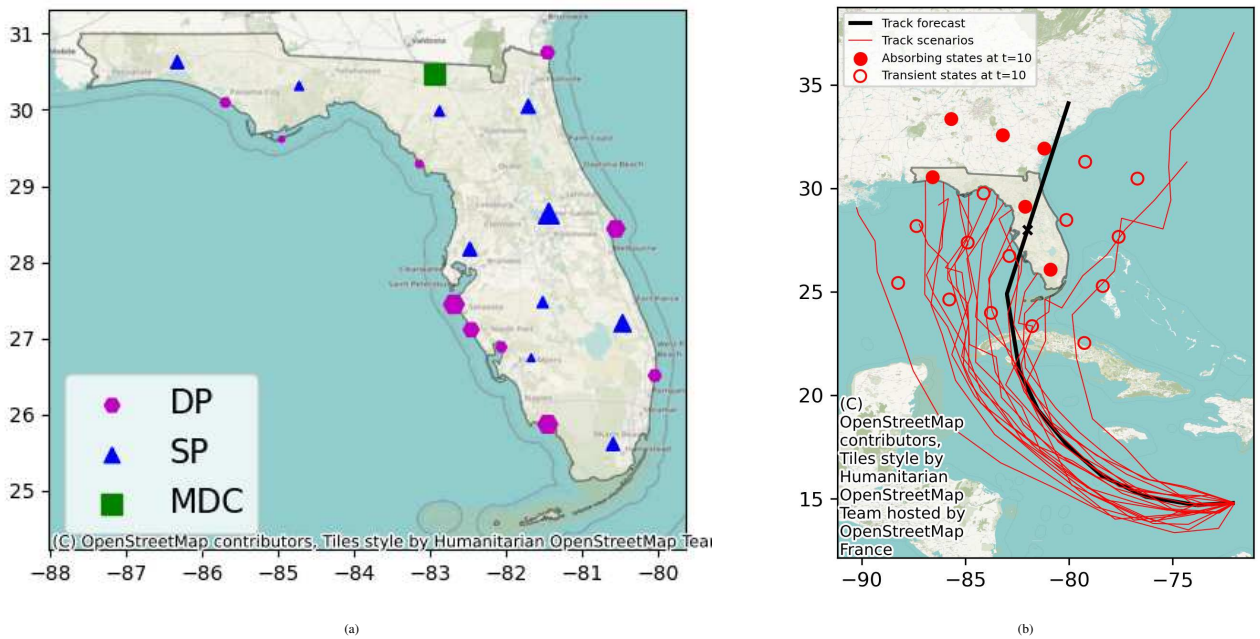

(a) (b)

FIGURE 3 An illustration of locations (of DPs, SPs, and the MDC), hurricane scenarios, and MC discretization for Hurricane Ian case study. The sizes of the markers representing SPs/DPs are proportional to their capacity and demand levels, respectively.

5.3.2 | Hurricane scenario generation

Hurricane scenarios are generated by using the point track and intensity forecast with along, cross, and intensity FE samples. Given the point forecast, a random realization of the along and cross errors may result in a sample path that terminates at an in-land location, i.e., it does not necessarily terminate on the coast line. Since the landfall of the hurricane is defined as the first time it reaches the land, we approximate the location of the last period of the sample path to be the intersection of the hurricane track and the coastline. An example of the hurricane's track scenarios is shown in Figure 3b. The Markovian states depicted in the figure will be explained in detail in Section 5.4.

5.3.3 | Demand estimation

Similar to the Florence case, the demand (D_{i,ξ_t}) of DP i at each time t is a function of distance between the DP and the hurricane location, hurricane intensity, and the time until the hurricane's landfall. When the hurricane's landfall time is random, as is the case for the Hurricane Ian case study, the time until the hurricane's landfall is a random variable. We thereby define the demand at a period to depend on hurricane track, intensity, and the expected time until landfall. The expected time until landfall

for any transient Markovian state ($\mathbb{E}[t_s]$) is computed based on the transition probabilities associated with the MC, or can be estimated empirically as the average landfall period of a number of randomly generated scenarios, using the error realizations of the sample path at t. Specifically, in equation (14), the demand realization according to lead time (D^{τ}_{i,ξ_t}) and location (D^{loc}_{i,ξ_t}) is computed as $\left(1 - \frac{\mathbb{E}[t_s]-t}{\tau}\right)$, and $\left(1 - \frac{\|\xi_{t,x,y}-L_i\|}{x_{\max}}\right)$, respectively.

5.4 | Markov chain discretization

The forecast error (FE) samples derived from the AR-1 models offer a means to generate demand estimates applicable directly to 2SSP models. For modeling the MSSP, we approximate the hurricane process as an MC, a concept alternatively described through the policy graph framework introduced in [20].

Specifically, recall that we denote the FEs as $\xi_t := (\xi^T, \xi^I_t)$ for the Hurricane Florence case and $\xi_t := (\xi^A, \xi^C_t, \xi^I_t)$ for the Hurricane Ian case. Here, ξ^T, ξ^A, ξ^C_t, and ξ^I_t correspond to the error realizations of track, along, cross, and intensity FEs, respectively. We note that ξ^T represents the one-dimensional track error, which, when combined with the track point forecast, yields the respective location $(\xi_{t,x}, \xi_{t,y})$. Similarly, overlaying the along and cross forecast errors (ξ^A_t, ξ^C_t) onto the point track forecast provides the location $(\xi_{t,x}, \xi_{t,y})$. In the Florence case, all states at the final stage are classified as absorbing, while in the Ian case, the Markovian states are characterized as either absorbing or transient based on the associated location information.

We now discuss how to construct an MC discretization for the MSSP according to a set of FE scenarios sampled from the AR-1 models. For the state space of the MC on hurricane intensity, we use the Saffir-Simpson scale given by: $\{0, 1, \cdots, 5\}$. We construct the transition probability matrix of the MC on intensity using the empirical probability distribution according to 10000 randomly generated intensity scenarios from the AR-1 FE model of intensity, converted into their respective hurricane categories. To construct an MC discretization for hurricane's location, we perform an MC discretization on the FEs first, and then overlay the discretized FEs onto the track point forecast to obtain the Markovian states related to locations. Finally, based on the obtained location information associated with the Markovian states, we classify them as either transient or absorbing states. We next discuss the detailed discretization technique for the track, along, and cross FEs into MCs and obtaining the corresponding transition probability matrix.

5.4.1 | Discretization of forecast errors

We adopt the MC discretization technique proposed by [33]. Specifically, let $[\xi_{t,s}]_{s=1}^{S_t}$ represent the set of Markovian states at stage t, and the collection of $\{[\xi_{1,s}]_{s=1}^{S_1}, \cdots, [\xi_{T,s}]_{s=1}^{S_T}\}$ represents the state space of the MC lattice. Given a sequence of random vectors $\{\eta_t\}_{t=1}^{T}$ with probability distribution P, the optimal discretization at each stage t can be obtained by solving the following optimization problem.

$$\min_{\{\xi_{t,s}\}_{s=1}^{S_t}} \int \min_{s=1,\cdots,S_t} \|\eta_t - \xi_{t,s}\| dP(\eta_t) \tag{15}$$

Problem (15) is known to be NP-hard, and an approximate solution can be obtained by the approach of sample average approximation (SAA) [33]. In SAA, we randomly draw samples from the FE's distribution and update the discretization points $\{\xi_{t,s}\}_{s=1}^{S_t}$. The n^{th} sample drawn is assigned to the nearest discretization point from the $(n-1)^{th}$ iteration. The initialization conditions are chosen arbitrarily. The updating rule is as follows:

$$\xi^n_{t,s} = \begin{cases} \xi^{n-1}_{t,s} + \beta_k(\hat{\eta}^n_t - \xi^{n-1}_{t,s}), \text{if s} = \arg\min_{s'=1,\cdots,S_t}\{\|\hat{\eta}^n_t - \xi^{n-1}_{t,s'}\|\} \\ \xi^{n-1}_{t,s}, \text{ otherwise} \end{cases}$$

As a result of the iterations above, the final discretized states after training with N samples are $\xi_{t,s} = \xi^N_{t,s}, \forall s = 1, \cdots S_t, \forall t = 1, \cdots, T$. The sets of all random samples, $\{\hat{\eta}^n_t\}_{n=1}^{N}$ that are closest to the respective $\xi_{t,s}$, $\forall s = 1, \cdots, S_t, \forall t = 1, \cdots, T$ are represented by $\Gamma_{\xi_{t,s}}$ and can be used to compute the transition probabilities between the Markovian states as follows:

$$p_{\xi_{t,s},\xi_{t+1,s'}} = \frac{\sum_{n=1}^{N} \mathbb{I}_{\Gamma_{\xi_{t,s}}}(\hat{\eta}^n_t) \times \mathbb{I}_{\Gamma_{\xi_{t+1,s'}}}(\hat{\eta}^n_{t+1})}{\sum_{n=1}^{N} \mathbb{I}_{\Gamma_{\xi_{t,s}}}(\hat{\eta}^n_t)}; \ \forall s = 1, \cdots, S_t, \forall s' = 1, \cdots, S_{t+1}, t = 1, \cdots, T-1 \tag{16}$$

where $\mathbb{I}_{\Gamma_{\xi_{t,s}}}(\hat{\eta}^n_t)$ is an indicator function that represents whether or not training sample $\hat{\eta}^n_t$ at period t is in set $\Gamma_{\xi_{t,s}}$.

We use 10000 randomly generated scenarios to train the MC discretization model for track, along, and cross FEs, respectively. Since the number of Markovian states at a period is inversely proportional to the total discretization loss, the larger number of Markovian states used, the better representation for the data process is achieved. However, a large number of Markovian states will lead to high computational effort for solving the MSSP model. To keep it computationally more viable, we start by using a predefined number of Markovian states at $t = T$: we set 10 states for the track error and five states each for along and cross errors. We then compute the average discretization error over the states at $t = T$ and use it as the discretization error threshold. Then, for each period $t < T$, we choose the maximum number of states that the corresponding discretization error falls below this threshold. An example for discretization of track error is presented in Figure A11 in the Appendix. We define sets Ξ_t^T, Ξ_t^A, and Ξ_t^C as the the discretized MC state space of track, along, and cross FEs.

5.4.2 | Generation of the MC model for MSSP from the discretized forecast errors

The MC model for MSSP is constructed by combining the MC state spaces of intensity and track scenarios, each represented by independent MC processes. Recall that at each period $t \in \mathcal{T}$, the state space of MC state on intensity, denoted as Ξ^I, consists of hurricane categories $\{0, 1, \cdots, 5\}$. Similarly, the state spaces of MC states on track, along, and cross FEs, denoted as Ξ_t^T, Ξ_t^A, and Ξ_t^C, respectively, are described in the previous section. For the Hurricane Florence case study, we then overlay Ξ_t^T onto the point track forecast to obtain the state space Ξ_t^L of MC state on hurricane's location, i.e., each pair $(\xi_{t,x}, \xi_{t,y}) \in \Xi_t^L$ represents the hurricane location state. Similarly, for the Hurricane Ian case study, we overlay Ξ_t^A and Ξ_t^C onto the point track forecast to obtain the MC state on hurricane's location. The illustrations of the MC states on Hurricane Florence and Hurricane Ian are shown in Figure 2b and Figure 3b, respectively, and the numbers of Markovian states used in the Hurricane Florence and Hurricane Ian in each period are provided in Table A3 and Table A4 in the Appendix, respectively. Furthermore, for Hurricane Ian case study, all hurricane states at $t = T$ and states at $t < T$ that represent inland locations or are within five miles from the coastline are categorized as absorbing states. All other states are categorized as transient states.

5.5 | Logistics cost parameters

In our numerical experiment, we adapt the generation of the logistics cost parameters for both of our case studies from [17] with some modifications as shown on Table 2.

TABLE 2 Description of logistics cost parameters used in the numerical experiments.

Parameter description	Notation	Value
One-time setup cost of SP	c_j^F	$q_j \times \kappa^F$
Keep-up cost (per period) of an active SP	c_j^f	$c_j^F \times \kappa^f; \kappa^f = 0.1$
Unit inventory cost of relief items in SP	c_j^{InvR}	$c^P \times \kappa^{InvR}; \kappa^{InvR} = 0.1$
Unit relief handling cost per evacuee in SP	c_j^{InvE}	$c^P \times \kappa^{InvE}; \kappa^{InvE} = 0.1$
Unit cost of emergency relief items shipped to SP	c_j^G	$c^P + c_{0,j}^R \times \kappa^G; \kappa^G = 100$
Unit cost for unused relief items to be shipped out of SP	c_j^H	$-c^P \times \kappa^H; \kappa^H = 0.1$
Unit evacuation cost of evacuees	c_{ij}^E	$d_{i,j} \times \kappa^{distE}; \kappa^{distE} = 0.1$
Unit transportation cost of relief items	$c_{j',j}^R$	$d_{j',j} \times \kappa^{distR}; \kappa^{distE} = 0.01$
Amount of relief items needed per evacuee per period	ϕ	1

The hyper-parameters κ's (with various superscripts) in Table 2 are the cost factors associated with the respective cost parameters. The values of κ's magnify the corresponding logistics cost parameters in a linear fashion. The estimation of hyper-parameters κ's can be regulated by historical disaster logistics observations. In our experiments, due to lack of historical data, we randomly pick the values suitable for our model, and we analyze the impact of different values of κ^F, κ^{PE}, and c^P parameters through sensitivity analyses in Section 6.

5.6 | Out-of-sample experiment setup

In this section, we describe our out-of-sample experiment setup to evaluate the out-of-sample performance of the decision policies obtained from the MSSP models and the 2SSP-based approaches. We emphasize that the hurricane scenarios that are used for solving the MSSP and 2SSP models are referred to as the *in-sample* scenarios. A hurricane scenario that is obtained from overlaying a sample of the FEs (from the AR-1 models with the same parameter specification) on the initial point forecast is referred to as an *out-of-sample* (OOS) scenario. Either the sample average approximation (SAA) used in 2SSP-based approaches or the MC discretization used in MSSP models only provides us a set of decision policies defined (and trained) on the given in-sample scenarios. An OOS experiment to analyze the cost of a decision policy over a set of OOS scenarios is necessary to test the actual performance of the decision policies trained from the in-sample scenarios. Given an MC disretization with state space Ξ_t, $\forall t \in \mathcal{T}$, the fully adaptive decision policy associated with the MSSP is well-defined. We conduct an OOS test for the performance of the optimal policies over a collection of OOS scenarios sampled from the discretized MC model, which we refer to as the *OOS scenarios from the MC*. Additionally, we conduct an OOS test on the OOS scenarios sampled from the AR-1 models for the FEs, which we refer to as the *true OOS scenarios*, to compute the value of the optimal policies trained by the MSSP model on the discretized MC.

5.6.1 | OOS test of the MSSP model on true OOS scenarios

MSSP models are optimized over a recombining scenario tree defined by the MC model, where each transient Markovian state is associated with an expected CTG function trained through the SDDP algorithm. After running the SDDP algorithm, we retrieve the optimal first-stage solution and the trained expected CTG functions associated with all the transient Markovian states and use them in the OOS test. The total cost along an OOS scenario from the MC can be computed by utilizing the expected CTG functions associated with the Markovian states on this OOS scenario. However, the OOS test on a true OOS scenario cannot be done in the same manner since the hurricane states on the true OOS scenario may not correspond to any Markovian state. Having a good policy to pick the right expected CTG function for each state along the true OOS scenario is crucial to minimize the performance discrepancy between training (in-sample performance) and testing (out-of-sample performance). We proceed by describing the policies we use in our case studies.

OOS test in Hurricane Florence case study

Given a true OOS scenario $\{\eta_1, \cdots, \eta_T\}$, at each period $t = 2, 3, \cdots, T$, we adopt the decision policy induced by the expected CTG function (trained from the SDDP algorithm) associated with the Markovian state that is closest to η_t, based on a certain metric. Specifically, let (η_t^I, η_t^T) denote the hurricane's intensity (represented in the SS scale) and track information associated with η_t. Recall that every Markovian state $\xi_t \in \Xi_t$ is represented by the respective hurricane intensity and track attributes: $\xi_t = (\xi_t^I, \xi_t^T)$. To determine the closest Markovian state $\tilde{\xi}_t \in \Xi_t$ to η_t, we select $\tilde{\xi}_t^I$ such that $\tilde{\xi}_t^I \in \arg\min\{|\xi_t^I - \eta_t^I| : \xi_t \in \Xi_t\}$ and $\tilde{\xi}_t^T$ such that $\tilde{\xi}_t^T \in \arg\min\{|\xi_t^T - \eta_t^T| : \xi_t \in \Xi_t\}$. We then select the expected CTG function associated with $\tilde{\xi}_t := (\tilde{\xi}_t^I, \tilde{\xi}_t^T)$, which is given by $\mathcal{Q}_{t+1}^{\xi_t}(\cdot)$, and solve it using the OOS data η_t.

OOS test in Hurricane Ian case study

The assumption of random landfall time in the Hurricane Ian case study makes the approach for OOS test on the true OOS scenarios slightly different than the Florence case. Let $\{\eta_1, \cdots, \eta_{t_s}\}$ be an OOS scenario where $t_s \leq T$ represents the terminal stage of the OOS scenario. Unlike in Florence case, the hurricane track scenarios in this case are characterized by along and cross FEs. For a given OOS state $\eta_t := (\eta_t^I, \eta_t^A, \eta_t^C)$, our objective is to select the expected CTG function associated with the state $\tilde{\xi}_t = (\tilde{\xi}_t^I, \tilde{\xi}_t^A, \tilde{\xi}_t^C)$ that is closest to η_t. To achieve this, we proceed by selecting $\tilde{\xi}_t^I \in \arg\min\{|\xi_t^I - \eta_t^I| : \xi_t \in \Xi_t\}$, followed by $\tilde{\xi}_t^A \in \arg\min\{|\xi_t^A - \eta_t^A| : \xi_t \in \Xi_t\}$, and $\tilde{\xi}_t^C \in \arg\min\{|\xi_t^C - \eta_t^C| : \xi_t \in \Xi_t\}$, in this specific order. We denote the closest Markovian state $\tilde{\xi}_t \in \Xi_t$ to η_t, calculated using the described steps, as $\tilde{\xi}_t \in \arg\min\{\|\xi_t - \eta_t\| : \xi_t \in \Xi_t\}$. However, the expected CTG function that we pick this way may be associated with an absorbing state for $t < t_s$, or associated with a transient state for $t = t_s$. Since a sample path is characterized as a sequence of transient states followed by an absorbing state at the termination, we modify the policy for picking the expected CTG functions using the following two heuristics:

H1 Define a set of sequence of hurricane states from the MC model that are closest to the OOS states: $S^{H1} = \{\tilde{\xi}_t : \tilde{\xi}_t \in \arg\min\{\|\xi_t - \eta_t\| : \xi_t \in \Xi_t, t = 1, \cdots, t_s\}$. Define $\bar{t}_s = \arg\min_t\{\xi_t \in S^{H1} : \xi_t \text{ is absorbing}\}$. Solve a sequence of CTG functions $Q_t^{\xi_t}(\hat{X}_{t-1}, \hat{z}, \eta_t) : \xi_t \in S^{H1}$ for $t < \bar{t}_s$ followed by the sequence of cost functions $Q_{t_s}(\hat{X}_{t_s-1}, \hat{z}, \xi_{t_s}) : \mathcal{Q}_{t_s+1}(\cdot) = 0$ for $t \in \{\bar{t}_s, \cdots, t_s\}$.

H2 For all $t < t_s$, pick the expected CTG function associated with state $\tilde{\xi}_t$ such that $\tilde{\xi}_t \in \arg\min\{\|\xi_t - \eta_t\| : \xi_t \in \Xi_t,\ \xi_t \text{ is transient}\}$; for $t = t_s$, set the expected CTG function to be $\mathcal{Q}_{t_s+1}(\cdot) \equiv 0$ in the OOS test.

In terms of the selection of the expected CTG functions, heuristic H2 is similar to Florence case. However, in the presence of non-terminal absorbing states with the minimum distance to transient OOS states, the demand after the absorbing state should be satisfied locally without considering future cost. This may result into an expensive cost of a true OOS scenario. Hence going from the deterministic to random landfall case, it is critical to find an appropriate policy for choosing the expected CTG function in the OOS test with true OOS scenarios. We will demonstrate this with numerical results in Section 6.

5.6.2 | OOS test of the 2SSP model

An optimal solution to the 2SSP model solved at $t = 1$ provides a static decision policy, which corresponds to a set of first-stage decisions that are made before the hurricane uncertainty is unfolded. Since the recourse decisions of the proposed 2SSP model only include those associated with the in-sample scenarios, the recourse policy for any arbitrary OOS may not be readily available. Hence, given a first-stage decision, to compute the cost of a static decision policy from the 2SSP model on an OOS scenario, we need to apply certain policies to define the recourse decisions. Recall that our 2SSP subproblem (9) takes the entire sample path information $\{\eta_1, \cdots, \eta_{t_s}\}$ to optimize the recourse policy because of variables e_j's that link all periods together are treated as recourse variables instead of the first-stage variables. One policy is to supply the entire OOS scenario data and solve the second-stage subproblem (9) with the optimal first-stage solution to find the corresponding optimal recourse decision for the OOS scenario. We refer to this policy as *2SSP-anticipative*. We note that the 2SSP-anticipative policy is not implementable in practice, since at any period, an implementable policy should only take into consideration the information available up to that period and not the future, but it is useful in our benchmark to provide an optimistic bound on the 2SSP solution. On the other hand, we employ an implementable myopic heuristic approach that we refer to as *2SSP-myopic*, in which given the first-stage solution and the OOS scenario, we sequentially solve a deterministic problem at every period to determine the optimal recourse decision for that period only. Specifically, for given first-stage solutions, $(\hat{z}, \hat{\ell})$ and the OOS data $\{\eta_1, \cdots, \eta_{t_s}\}$, we solve deterministic optimization problem (17) at every period $t = 2, \cdots, t_s$ by utilizing the initial conditions $(\hat{e}_{t-1})$ and uncertainty realization D_{η_t} to determine the local decisions, $y_t, e_t, x_t, g_t, h_t, u_t$, and update the initial conditions for the next period. At $t = 1$, the initial conditions are $\hat{e}_{i,0} = \bar{D}_i,\ \forall i \in I$, $\hat{e}_{j,0} = 0,\ \forall j \in J$.

$$\min \sum_{i\in I}\sum_{j\in J} c^E_{i,j} y_{i,j,t} + \sum_{j\in J} c^{InvE}_j e_{j,t} + \sum_{j\in J}(c^P + c^R_{0,j})x_{0,j,t} + \sum_{j\in J}\sum_{j'\in J} c^R_{j,j'} x_{j,j',t} + \sum_{j\in J} c^G_j g_{j,t} + \sum_{j\in J} c^H_j h_{j,t} + \sum_{i\in I} c^{PE}_i u_{i,t} \tag{17a}$$

$$\text{s.t.} \sum_{j\in J} y_{i,j,t} + u_{i,t} = D_{i,\eta_t}\hat{e}_{i,t-1},\ \forall i \in I \tag{17b}$$

$$e_{i,t} = \hat{e}_{i,t-1} - \sum_{j\in J} y_{i,j,t},\ \forall i \in I \tag{17c}$$

$$e_{j,t} = \hat{e}_{j,t-1} + \sum_{i\in I} y_{i,j,t},\ \forall j \in J \tag{17d}$$

$$e_{j,t} \le q_j \hat{z}_j,\ \forall j \in J \tag{17e}$$

$$\hat{\ell}_{j,t-1} + x_{0,j,t} + \sum_{j'\in J, j\neq j'} x_{j',j,t} - \sum_{j'\in J, j\neq j'} x_{j,j',t} - \phi e_{j,t} + g_{j,t} - h_{j,t} = \hat{\ell}_{j,t}, \forall j \in J \tag{17f}$$

$$\sum_{j'\in J, j\neq j'} x_{j,j',t} \le \hat{\ell}_{j,t-1} + g_{j,t} - \phi e_{j,t},\ \forall j \in J \tag{17g}$$

$$\hat{\ell}_{j,t-1} + g_{j,t} - \phi e_{j,t} \le \phi q_j \hat{z}_j, \forall j \in J \tag{17h}$$

$$u_{i,t}, e_{i,t} \ge 0,\ \forall i \in I \tag{17i}$$

$$y_{i,j,t} \ge 0,\ \forall i \in I,\ \forall j \in J \tag{17j}$$

$$x_{j,j',t} \ge 0,\ \forall j \in J \cup \{0\},\ \forall j' \in J : j \neq j' \tag{17k}$$

$$e_{j,t}, g_{j,t}, g_{j,t} \geq 0, \ \forall j \in J \tag{17l}$$

5.7 | Implementation details

The first-stage problem in MSSP and 2SSP models is a mixed-integer linear programming (MILP) problem. One approach to add cuts to the first-stage problem in Benders and SDDP algorithms is to solve the first-stage problem to optimality at every iteration and add cuts (10) and (13) generated with the optimal first-stage solution, which we refer to as the *simple Benders/SDDP* approach. However, in the presence of large number of integer variables, solving first-stage MILP problem to optimality at every iteration can be computationally expensive. In such cases, an alternative approach is to add cuts to the incumbent solution of the branch-and-bound tree of the first-stage MILP problem in *lazy* fashion. We refer to this approach as *branch-and-cut (BC) with lazy constraints*. Through our initial experiments, BC with lazy constraints is found to be more efficient than the simple Benders approach for the 2SSP models. However, for SDDP, BC with lazy constraints does not produce better results compared to the simple SDDP. We thereby use BC with lazy constraints for static 2SSP and simple SDDP to solve MSSP models.

We set the time limit of six hours for solving each instance in all our experiments. We set the cut violation threshold to 10^{-5} in the cutting plane generation. The termination criterion of the SDDP algorithm is regulated by a lower bound improvement threshold in which we stop the SDDP algorithm if the relative gap between the lower bounds in 1000 subsequent iterations is less than $\tau = 10^{-3}$ or the time limit is reached. At the time of termination, we report the statistical upper bound computed with $M = 10000$ sample paths. All the implementations are done in Python 3, utilizing the Gurobi optimization solver version 10.0 on Palmetto cluster, a high performance computing cluster at Clemson University, with 2.60GHz, 64 cores processor, and 128GB memory.

6 | NUMERICAL RESULTS AND DISCUSSION

In this section, we present numerical results from our experiments. As mentioned in Sections 5.2 and 5.3, we consider an integrated evacuation and logistics network with $|I| = |J| = 10$ in both case studies. We create instances with different parameters by varying the values of κ^F, κ^{PE}, and c^P as mentioned in Section 5.5. We refer to a combination of κ^F, κ^{PE}, and c^P as a *cost configuration*. We create a baseline instance with $\kappa^F = 5, \kappa^{PE} = 200$, and $c^P = 5$ and we use it as the basis for comparing with other configurations. Since we are interested in analyzing the impact of each cost parameter to the results, we change the value of one parameter at a time while keeping the other two the same as the base model through a sensitivity analysis (SA). For the SA of the fixed cost, we pick different values of $\kappa^F \in \{1, 10, 20, 50\}$ while keeping the values of κ^{PE} and c^P the same as the base model and report the corresponding results. The SA of the penalty and purchase cost are done in a similar manner with instances created with $\kappa^{PE} \in \{50, 100, 300, 500\}$, and $c^P \in \{1, 10, 50, 100\}$, respectively. These settings altogether give us 13 cost configurations for each case study. The ranges of κ^F, κ^{PE}, and c^P are chosen to represent the respective cost parameter's low to high ends. The lower end of κ^{PE} is determined based on the principle that the unit penalty for not meeting evacuation demand, on average, should surpass the costs linked with providing the corresponding amount of relief commodities, including procurement, transportation, and inventory, as well as emergency procurement costs.

In each case study, we provide an analysis of three key components: the first-stage SP activation decisions, the performance of the algorithms employed, and the OOS test results. The latter two aspects are examined across the aforementioned 13 different cost configurations. Additionally, we utilize an in-sample scenario size of $|S| = 100$ for solving the 2SSP models in both case studies. This determination is based on the outcomes of our preliminary experiments, which have indicated that this sample size is sufficient from the in-sample stability perspective. In the tables to be shown later in this section, we use the following abbreviations.

6.1 | Case study on Hurricane Florence

In the Hurricane Florence case study, we assume a time horizon of $|\mathcal{T}| = 11$, where all the Markovian states are absorbing at $t = 11$, and all other states are transient. Table 4 presents the results of the SDDP and Benders decomposition algorithms for solving the MSSP model and 2SSP model in the Hurricane Florence case study, respectively. Within the time limit of six

TABLE 3 Abbreviations used in result tables.

Name	Description
Time	Computational time in seconds
# Nodes	Number of nodes explored in the branch-and-bound tree of the 2SSP master problem
# Iterations	Number of iterations of the SDDP algorithm until termination
LB	The lower bound provided by the SDDP algorithm at termination
UB^+	$UB^+ := \bar{\mu} + 1.96 \times \frac{\bar{\sigma}}{\sqrt{M}}; M = 10000$. The upper confidence limit of the statistical UB of the SDDP at termination
Gap	Gap $:= \frac{UB^+ - LB}{UB^+} \times 100\%$, the relative gap (in percentage) between the LB and UB^+ provided by the SDDP algorithm
CI of obj	CI$:= \bar{\mu} \pm 1.96 \times \frac{\bar{\sigma}}{\sqrt{M}}; M = 10000$. 95% confidence interval of the objective in the OOS test
P-GAP	Performance gap in terms of the objective value (in percentage) between the MSSP model and the 2SSP models
2-A/2-M/MS	2SSP-anticipative/2SSP-myopic/MSSP

hours, the Benders decomposition algorithm terminates with an optimal solution to the 2SSP model, while the SDDP algorithm converges to a low gap (< 2%) between the lower bound and the statistical upper bound. The computational time of the SDDP algorithm is 2.42 times more, on average, than the Benders decomposition algorithm.

TABLE 4 Algorithm results for Hurricane Florence case study.

			Benders decomposition for 2SSP			SDDP for MSSP				
κ^F	κ^{PE}	c^P	**Objective**	**Time**	**# Nodes**	**LB**	**UB^+**	**Gap**	**Time**	**# Iterations**
5	200	5	1.99×10^6	6737.83	4211	1.91×10^6	1.93×10^6	0.99%	14857.63	2898
1	200	5	1.35×10^6	5732.77	4581	1.27×10^6	1.29×10^6	1.59%	18089.16	3232
10	200	5	2.76×10^6	7551.95	4667	2.69×10^6	2.71×10^6	0.96%	14863.41	2850
20	200	5	4.27×10^6	5545.95	3663	4.20×10^6	4.24×10^6	0.95%	13086.34	2631
50	200	5	8.52×10^6	4821.06	3407	8.47×10^6	8.55×10^6	1.04%	9385.49	2177
5	50	5	1.95×10^6	5155.38	4125	1.88×10^6	1.88×10^6	0.34%	21602.84	3471
5	100	5	1.98×10^6	6811.09	4337	1.90×10^6	1.92×10^6	1.11%	19216.16	3288
5	300	5	1.99×10^6	6797.05	4272	1.91×10^6	1.92×10^6	0.70%	13412.19	2769
5	500	5	1.99×10^6	5829.71	3792	1.92×10^6	1.93×10^6	0.70%	14553.34	2860
5	200	1	1.09×10^6	6360.30	4258	1.07×10^6	1.08×10^6	0.77%	13678.55	2745
5	200	10	3.07×10^6	7584.86	4476	2.92×10^6	2.97×10^6	1.62%	10233.64	2377
5	200	50	1.11×10^7	3871.23	3504	1.09×10^7	1.10×10^7	0.64%	5209.70	1625
5	200	100	1.73×10^7	1314.11	2344	1.73×10^7	1.73×10^7	0.31%	21603.99	4397

6.1.1 | Shelters activation decision

Figure 4 illustrates the activation decisions of SPs in the base configuration of both the 2SSP and MSSP models for the Florence case study. Given that SPs are activated at $t = 1$ based on the first-stage decision, the decisions regarding shelter openings are notably similar between the two models across all instances. The activation of SPs is influenced by various factors, including their distances from the MDC and DPs, their capacities, and the associated fixed costs.

The MSSP model incorporates adaptive decision-making for the inventory levels of relief items, whereas the 2SSP model relies solely on a static first-stage solution. Consequently, in the MSSP model, where inventory levels can be adjusted according to demand realizations, the emergency relief commodity transportation is minimized to the most extent. Thus the activation decisions of SPs in the MSSP model are more influenced by the evacuation costs. Conversely, in the 2SSP model, optimized with an entire sample path information but with non-adaptive relief inventory decisions, the emergency relief items transportation cost cannot be avoided to meet inventory requirements in various scenarios. Due to this non-adaptive nature, the activation decisions of SPs in the 2SSP model are equally influenced by the relief commodity transportation cost and evacuation cost, resulting in SP activation based on the proximity to the MDC as well. Nonetheless, SPs with higher capacities and lower evacuation costs are activated in both models due to significant cost savings, irrespective of the adaptiveness of the model.

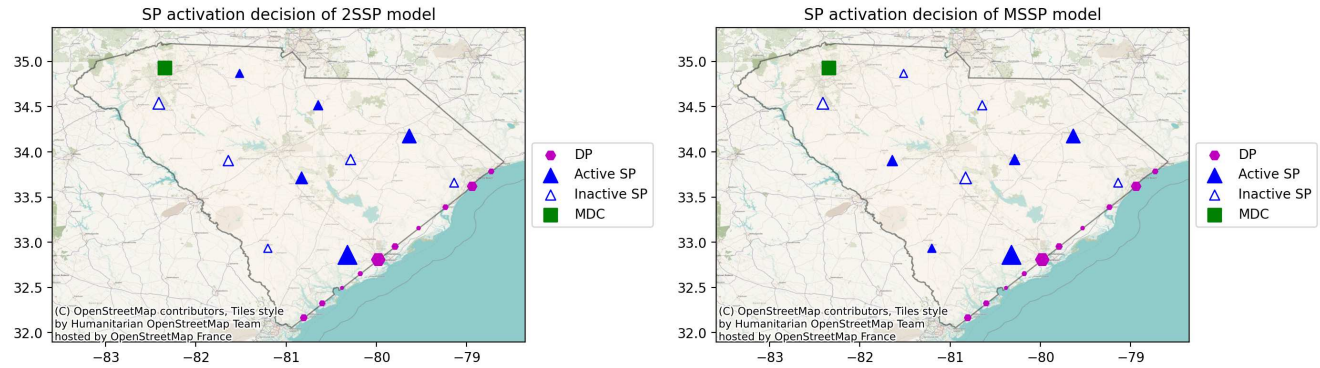

FIGURE 4 Activation of SPs in Florence case study for $\kappa^F = 5$, $\kappa^{PE} = 200$, $c^P = 5$.

6.1.2 | OOS performance

In this section, we examine the performance of static and adaptive policies through OOS testing, utilizing scenarios generated from MC model and true OOS scenarios. Tables 5 and 6 provide the average cost with 95% confidence intervals (CIs) for the MSSP model, 2SSP-anticipative, and 2SSP-myopic.

TABLE 5 OOS test results of Florence case study on OOS scenarios from the MC model.

			MSSP	2SSP-anticipative		2SSP-myopic	
κ^F	κ^{PE}	c^P	CI of obj	CI of obj	P-Gap	CI of obj	P-Gap
5	200	5	$1.93 \times 10^6 \pm 8.17 \times 10^3$	$1.99 \times 10^6 \pm 8.59 \times 10^3$	3.35%	$3.05 \times 10^6 \pm 1.36 \times 10^4$	36.69%
1	200	5	$1.30 \times 10^6 \pm 7.41 \times 10^3$	$1.34 \times 10^6 \pm 6.16 \times 10^3$	2.75%	$2.38 \times 10^6 \pm 1.19 \times 10^4$	45.34%
10	200	5	$2.73 \times 10^6 \pm 8.72 \times 10^3$	$2.76 \times 10^6 \pm 8.97 \times 10^3$	1.62%	$3.78 \times 10^6 \pm 1.38 \times 10^4$	28.17%
20	200	5	$4.25 \times 10^6 \pm 1.28 \times 10^4$	$4.29 \times 10^6 \pm 1.38 \times 10^4$	1.02%	$5.31 \times 10^6 \pm 1.77 \times 10^4$	19.88%
50	200	5	$8.50 \times 10^6 \pm 2.17 \times 10^4$	$8.55 \times 10^6 \pm 2.46 \times 10^4$	0.57%	$9.53 \times 10^6 \pm 2.77 \times 10^4$	10.78%
5	50	5	$1.89 \times 10^6 \pm 8.25 \times 10^3$	$1.94 \times 10^6 \pm 7.62 \times 10^3$	2.73%	$2.95 \times 10^6 \pm 1.26 \times 10^4$	36.00%
5	100	5	$1.93 \times 10^6 \pm 8.60 \times 10^3$	$1.96 \times 10^6 \pm 7.34 \times 10^3$	1.95%	$2.98 \times 10^6 \pm 1.26 \times 10^4$	35.46%
5	300	5	$1.92 \times 10^6 \pm 7.81 \times 10^3$	$2.00 \times 10^6 \pm 8.71 \times 10^3$	4.11%	$3.02 \times 10^6 \pm 1.36 \times 10^4$	36.44%
5	500	5	$1.93 \times 10^6 \pm 7.67 \times 10^3$	$1.99 \times 10^6 \pm 7.23 \times 10^3$	2.77%	$3.02 \times 10^6 \pm 1.26 \times 10^4$	36.05%
5	200	1	$1.08 \times 10^6 \pm 2.27 \times 10^3$	$1.11 \times 10^6 \pm 3.81 \times 10^3$	2.31%	$1.93 \times 10^6 \pm 7.84 \times 10^3$	44.04%
5	200	10	$2.94 \times 10^6 \pm 1.47 \times 10^4$	$3.07 \times 10^6 \pm 1.44 \times 10^4$	4.37%	$4.24 \times 10^6 \pm 1.95 \times 10^4$	30.76%
5	200	50	$1.06 \times 10^7 \pm 7.05 \times 10^4$	$1.11 \times 10^7 \pm 7.03 \times 10^4$	5.26%	$1.23 \times 10^7 \pm 7.19 \times 10^4$	13.97%
5	200	100	$1.74 \times 10^7 \pm 1.41 \times 10^5$	$1.75 \times 10^7 \pm 1.45 \times 10^5$	0.67%	$2.11 \times 10^7 \pm 1.43 \times 10^5$	17.62%

To begin with, the average MSSP cost, across all configurations, on true OOS scenarios is only 1.5% higher than the average cost of OOS scenarios from the MC model, indicating that the MC approximation effectively captures the characteristics of the underlying stochastic process. Across all cost configurations, the MSSP model exhibits better cost efficiency than 2SSP-anticipative and 2SSP-myopic with gaps 2.58% and 30.09%, respectively, for OOS scenarios generated from the MC model. Similarly, for true OOS scenarios, the gaps of 1.46% and 19.19% are observed, respectively. These consistent findings underscore the superior cost efficiency of the MSSP model compared to the 2SSP model in both test cases. Moreover, these results support the assertion that 2SSP-anticipative outperforms 2SSP-myopic due to its ability to optimize over the entire sample path with future evacuation decisions optimized at $t = 1$ because of its information advantage. On the other hand, even with this impractical information advantage, the 2SSP-anticipative is still outperformed by the MSSP policy by a significant margin, indicating the value of adaptability exhibited by the decision policy associated with the MSSP model. Additionally, the wider confidence interval (CI) for 2SSP-myopic compared to MSSP and 2SSP-anticipative indicates higher variability in its performance.

For the OOS test conducted over the OOS scenarios from the MC model, the MSSP model, being fully adaptive and optimized over the entire recombining tree of the MC model, outperforms the static 2SSP model. However, the gap between the MSSP model and static 2SSP model (in terms of both 2SSP-anticipative and 2SSP-myopic) narrows when testing over true

TABLE 6 OOS test results of Florence case study on the true OOS scenarios.

			MSSP	2SSP-anticipative		2SSP-myopic	
κ^F	κ^{PE}	c^P	CI of obj	CI of obj	P-Gap	CI of obj	P-Gap
5	200	5	$1.97 \times 10^6 \pm 4.55 \times 10^3$	$2.00 \times 10^6 \pm 6.45 \times 10^3$	1.77%	$2.93 \times 10^6 \pm 1.27 \times 10^4$	32.86%
1	200	5	$1.33 \times 10^6 \pm 4.11 \times 10^3$	$1.36 \times 10^6 \pm 6.34 \times 10^3$	1.95%	$2.33 \times 10^6 \pm 1.24 \times 10^4$	42.70%
10	200	5	$2.75 \times 10^6 \pm 4.82 \times 10^3$	$2.78 \times 10^6 \pm 6.89 \times 10^3$	1.07%	$3.71 \times 10^6 \pm 1.35 \times 10^4$	25.84%
20	200	5	$4.29 \times 10^6 \pm 6.98 \times 10^3$	$4.30 \times 10^6 \pm 8.69 \times 10^3$	0.30%	$5.29 \times 10^6 \pm 1.70 \times 10^4$	18.90%
50	200	5	$8.52 \times 10^6 \pm 1.17 \times 10^4$	$8.54 \times 10^6 \pm 1.50 \times 10^4$	0.30%	$9.48 \times 10^6 \pm 2.94 \times 10^4$	10.20%
5	50	5	$1.92 \times 10^6 \pm 4.56 \times 10^3$	$1.97 \times 10^6 \pm 6.75 \times 10^3$	2.27%	$2.95 \times 10^6 \pm 1.32 \times 10^4$	34.88%
5	100	5	$1.96 \times 10^6 \pm 4.75 \times 10^3$	$1.99 \times 10^6 \pm 6.50 \times 10^3$	1.48%	$2.92 \times 10^6 \pm 1.27 \times 10^4$	32.86%
5	300	5	$1.96 \times 10^6 \pm 4.37 \times 10^3$	$2.01 \times 10^6 \pm 6.58 \times 10^3$	2.46%	$2.96 \times 10^6 \pm 1.29 \times 10^4$	33.95%
5	500	5	$1.97 \times 10^6 \pm 4.30 \times 10^3$	$2.01 \times 10^6 \pm 6.68 \times 10^3$	2.29%	$2.98 \times 10^6 \pm 1.31 \times 10^4$	33.93%
5	200	1	$1.09 \times 10^6 \pm 1.28 \times 10^3$	$1.10 \times 10^6 \pm 3.83 \times 10^3$	1.02%	$1.94 \times 10^6 \pm 7.50 \times 10^3$	43.90%
5	200	10	$3.01 \times 10^6 \pm 8.16 \times 10^3$	$3.09 \times 10^6 \pm 9.85 \times 10^3$	2.64%	$3.98 \times 10^6 \pm 1.93 \times 10^4$	24.34%
5	200	50	$1.09 \times 10^7 \pm 3.89 \times 10^4$	$1.11 \times 10^7 \pm 4.11 \times 10^4$	2.01%	$1.17 \times 10^7 \pm 8.05 \times 10^4$	6.78%
5	200	100	$1.76 \times 10^7 \pm 7.77 \times 10^4$	$1.75 \times 10^7 \pm 7.85 \times 10^4$	-0.55%	$2.17 \times 10^7 \pm 1.54 \times 10^5$	18.95%

OOS scenarios. This is not surprising because the optimization of the static 2SSP model is done with a set of scenarios sampled directly from the underlying stochastic process (i.e., the AR-1 models), whereas the MSSP model is optimized over the MC approximation.

The breakdown of cost components for each model is detailed in Table 7. Analysis of the base configuration reveals that in MSSP, a higher proportion of costs is attributed to relief prepositioning (encompassing relief purchase and inventory) and fixed costs compared to the 2SSP model (both 2SSP-anticipative and 2SSP-myopic). Conversely, the emergency cost in the 2SSP model constitutes a larger proportion of the total cost than in the MSSP model. This difference highlights the efficacy of the MSSP model's fully adaptive relief inventory decision-making, facilitating more efficient demand satisfaction through regular inventory and reducing reliance on costly emergency transportation, which is more prevalent in the static 2SSP model due to its non-adaptive relief inventory decisions.

TABLE 7 Proportion of cost components, on average, of the OOS test on true OOS scenarios in Hurricane Florence case study.

			Fixed			Inventory			Penalty			Emergency			Relief Purchase			Transportation		
κ^F	κ^{PE}	c^P	MS	2-A	2-M	MS	2-A	2-M	MS	2-A	2-M	MS	2-A	2-M	MS	2-A	2-M	MS	2-A	2-M
5	200	5	40%	39%	27%	9%	8%	6%	1%	1%	1%	9%	10%	36%	38%	37%	28%	3%	3%	3%
1	200	5	13%	12%	7%	14%	13%	8%	0%	0%	0%	9%	14%	46%	60%	56%	36%	5%	5%	3%
10	200	5	56%	55%	41%	7%	6%	4%	2%	2%	1%	1%	7%	28%	32%	27%	22%	2%	3%	2%
20	200	5	68%	68%	56%	4%	4%	4%	4%	4%	3%	1%	3%	20%	20%	19%	16%	2%	2%	2%
50	200	5	80%	78%	70%	2%	2%	2%	7%	9%	8%	3%	2%	11%	8%	9%	8%	1%	0%	0%
5	50	5	38%	37%	25%	9%	10%	6%	2%	2%	1%	12%	8%	36%	36%	41%	29%	3%	3%	2%
5	100	5	39%	39%	26%	9%	9%	6%	2%	1%	1%	13%	10%	36%	34%	38%	28%	4%	3%	3%
5	300	5	41%	39%	27%	9%	8%	6%	1%	1%	1%	9%	10%	37%	38%	37%	28%	3%	3%	3%
5	500	5	41%	40%	27%	9%	8%	6%	0%	1%	1%	8%	10%	36%	39%	38%	28%	3%	3%	3%
5	200	1	73%	72%	41%	4%	4%	2%	1%	1%	1%	0%	1%	43%	17%	16%	10%	6%	5%	4%
5	200	10	26%	25%	20%	10%	10%	8%	1%	1%	1%	23%	24%	35%	38%	37%	35%	3%	3%	2%
5	200	50	5%	7%	7%	9%	7%	8%	6%	7%	0%	65%	78%	85%	14%	0%	0%	1%	1%	1%
5	200	100	4%	4%	3%	4%	4%	8%	50%	53%	3%	42%	39%	85%	0%	0%	0%	0%	0%	0%

In the context of evacuations, where evacuees at SPs receive relief items periodically throughout the planning horizon, the decision between evacuation and incurring penalty costs can be complex. Evacuees subject to penalty costs at a particular period are not guaranteed to be accounted for in future demand. Consequently, in certain scenarios, it may be more beneficial to incur a penalty once rather than evacuate, particularly if demand for relief items at SPs can be met through emergency transportation for the remaining periods due to lack of sufficient relief inventory. While 2SSP-anticipative optimizes policies across the entire sample path, effectively balancing this trade-off (although in an impractical fashion), the MSSP model incorporates future expected costs via its expected CTG function. Conversely, 2SSP-myopic prioritizes short-term (local) decisions, leading to a reliance on evacuation strategies to avoid immediate penalty costs. However, the lack of consideration for future demand results in increased reliance on emergency transportation in subsequent periods, leading to higher emergency costs and less cost efficiency overall.

Moving forward, we focus our discussion on the results of the sensitivity analysis for fixed, penalty, and purchase costs, particularly emphasizing insights drawn from the OOS test on true OOS scenarios, as similar conclusions can be derived for the results on OOS scenarios from the MC model.

6.1.2.1 | *Sensitivity analysis on fixed cost*

When $\kappa^F = 1$, the fixed costs incurred are minimal, as evidenced by the proportion of fixed costs shown in Table 7, thus making costs related to relief logistics and transportation more dominant. However, as κ^F increases, the fixed costs become the predominant component of the total cost. The MSSP model, with its adaptive relief logistics capabilities, sees relief logistics costs, including relief purchase, inventory, and transportation, as more dominant when κ^F takes smaller values. Moreover, it efficiently avoids expensive emergency costs thanks to its adaptive inventory levels. Conversely, the non-adaptive first-stage relief inventory in the 2SSP models leads to higher emergency costs to fulfill demand not met by the static inventory levels. Additionally, we also see that a higher fixed cost makes the evacuation cost more expensive, leading to a relatively larger accumulation of penalty costs. In this case, since the fixed cost primarily corresponds to the first-stage decisions of activating SPs, the MSSP model's relief logistics adaptability offers little advantage with a very large κ^F value.

6.1.2.2 | *Sensitivity analysis on penalty cost*

The sensitivity analysis for κ^{PE} yields consistent outcomes across the specified range. Table 6 demonstrates that average costs and performance gap for various κ^{PE} values remain similar across all models. Notably, penalty costs represent no more than 2% of the total cost across all κ^{PE} configurations (see Table 7). The chosen range of κ^{PE} ensures that penalty costs outweigh relief logistics costs on average. Evacuation is favored over paying high penalty costs when sufficient relief inventory is available at SPs. Conversely, in scenarios where the available relief inventory falls short of meeting the demand of relief items at SPs, evacuation still becomes the preferred option because the combined cost of emergency relief supply and evacuee transportation is set to be lower than the penalty cost of not evacuating. Successful evacuations, rather than penalty costs, predominantly meet evacuation demands, explaining the consistent results across different κ^{PE} values. Furthermore, unevacuated evacuees may contribute to demand estimates in subsequent periods. In hurricane scenarios with initially high demand during evacuation, a one-time penalty cost may prove more cost-efficient than continuous relief item supply costs. Consequently, some penalty costs may be incurred, particularly when κ^{PE} is low. Conversely, at maximum κ^{PE}, even a single-period penalty cost exceeds multi-period relief logistics costs, prompting more evacuations. Moreover, a higher evacuation rate with large κ^{PE} reduces emergency transportation costs in the MSSP model due to its adaptive relief inventory management. In contrast, the non-adaptive relief inventory in 2SSP-anticipative leads to emergency costs satisfying relief item demands at SPs. Additionally, emergency costs constitute a more significant component in 2SSP-myopic due to its myopic decision-making policy based solely on local costs.

6.1.2.3 | *Sensitivity analysis on purchase cost*

The purchase cost directly influences inventory and emergency costs (see Table 2). When c^P is at its lowest ($c^P = 1$), both the purchase and fixed costs become more dominant in MSSP and 2SSP-anticipative as shown in Table 7. Consequently, sufficient relief logistics pre-positioning is achieved, even in the static 2SSP model. Given that 2SSP-anticipative optimizes evacuation decisions with complete sample path information, costly penalty and emergency expenses are avoided due to the availability of adequate relief inventory. Consequently, MSSP's adaptability offers less advantage, resulting in lower performance gap compared to the case when $c^P = 10$. Conversely, when the purchase cost is at its highest ($c^P = 100$), relief item pre-positioning becomes expensive, leading to demand satisfaction through more frequent penalty and emergency costs. With high purchase costs, emergency costs also increase. Since all evacuees at SPs should receive relief items every period but evacuees accounted for demand in one period are not necessarily accounted for in subsequent periods, at high purchase costs, it becomes beneficial to anticipate future demand to avoid costly delivery of relief items to SPs early on. Given that MSSP optimizes evacuation decisions based on the expected CTG functions and 2SSP-anticipative optimizes based on complete scenario information, the overall cost of 2SSP-anticipative is lower than MSSP in the case of high purchase costs in the OOS test. On the other hand, as purchase and emergency costs become more dominant in all models when c^P is increased from 1 to 10, the performance gap relative to 2SSP-myopic decreases, as 2SSP-myopic efficiently optimizes local emergency costs. At $c^P = 50$, due to expensive relief purchases, most demand at SPs is met through emergency transportation, further reducing performance gap. However, at $c^P = 100$, due to the high costs associated with emergency and relief supplies, the optimal solution in 2SSP-myopic is to evacuate and pay emergency costs, which is more cost-effective than penalty costs locally. Consequently, emergency costs become dominant, resulting in an increase in the performance gap.

6.2 | Case study on Hurricane Ian

In this section, we focus on the results of our case study on Hurricane Ian, where the landfall time is assumed to be random with a planning horizon of $|\mathcal{T}| = 15$. The findings derived from the application of the Benders decomposition and SDDP algorithms across 13 model configurations are presented in Table 8. Notably, while the Benders decomposition algorithm attains optimality within the time limit of six hours, the SDDP algorithm terminates at an average gap of 9.2% at the time limit. The computational time required by the SDDP algorithm to reach this gap is, on average, 6.6 times longer than that of the 2SSP model. Furthermore, the average computational time of the SDDP algorithm across all cost configurations for the Ian case surpasses that of the corresponding Florence case by 41%, while the optimality gap in the Florence case remains below 2% for all configurations. This observation underscores the computationally demanding nature of the SDDP model for cases with random landfall time.

TABLE 8 Algorithm results for Hurricane Ian case study.

			Benders decomposition for 2SSP			SDDP for MSSP				
κ^F	κ^{PE}	c^P	**Objective**	**Time**	**# Nodes**	**LB**	**UB$^+$**	**Gap**	**Time**	**# Iterations**
5	200	5	2.97×10^7	3559.58	4022	2.48×10^7	2.76×10^7	10.02%	-	2739
1	200	5	2.23×10^7	2463.25	1796	1.76×10^7	1.92×10^7	8.46%	-	2495
10	200	5	3.86×10^7	4775.76	3974	3.37×10^7	3.66×10^7	7.96%	-	2278
20	200	5	5.52×10^7	3128.73	3377	5.08×10^7	5.65×10^7	10.11%	-	2367
50	200	5	9.99×10^7	3604.99	2977	9.68×10^7	1.01×10^8	4.57%	-	2356
5	50	5	2.84×10^7	5082.04	4648	2.43×10^7	2.64×10^7	8.00%	-	2348
5	100	5	2.94×10^7	5889.95	4890	2.46×10^7	2.76×10^7	10.62%	-	2366
5	300	5	2.99×10^7	3665.96	4827	2.48×10^7	2.87×10^7	13.59%	-	2336
5	500	5	3.00×10^7	4002.48	4605	2.50×10^7	2.92×10^7	14.66%	-	2386
5	200	1	1.93×10^7	5420.17	4585	1.74×10^7	1.91×10^7	9.06%	-	2392
5	200	10	4.23×10^7	3115.46	3424	3.40×10^7	3.84×10^7	11.46%	-	2290
5	200	50	1.34×10^8	2230.84	1321	1.07×10^8	1.15×10^8	6.91%	-	2442
5	200	100	1.68×10^8	299.90	654	1.57×10^8	1.63×10^8	4.14%	7991.75	1392

"-": The time limit of six hours is reached

Shelters activation

The activated shelters in the base configuration of both the 2SSP and MSSP models for the Ian case study are depicted in Figure 5. Notably, the number of activated SPs in the Ian case exceeds that of the Florence case. This difference can be attributed to the higher demand observed over a longer planning horizon in the Ian case compared to the Florence case. Similar to the Florence case, the decision of SP activation demonstrates a high level of similarity between the 2SSP and MSSP models in the Ian case, as this decision is made at the first stage in both models. Only two SPs exhibit different activation decisions between the two models, a phenomenon which can be explained similarly to the Florence case.

Performance of the heuristic policies for choosing the expected CTG functions in the OOS test

The OOS test in the Ian case can be conducted using two heuristics described in Section 5.6.1. The results of the OOS test for the base instance using 10000 true OOS scenarios, including a 95% CI of the average cost and the percentages of the cost components, are presented in Table 9 for both heuristics. We observe that the average OOS cost in the MSSP model with heuristic H1 is 31% lower than that with H2. Furthermore, the OOS objective value under H1 is only 3% higher than the in-sample objective value as seen in Table 8. It is noteworthy that the proportion of the total cost allocated to relief items prepositioning (including purchase, fixed, inventory, and transportation costs) is higher in H1 compared to H2, while the emergency cost is higher in H2. Furthermore, the proportions of cost components in the in-sample results and the OOS test results under heuristic H1 are similar. When employing H1, a series of expected CTG functions linked with transient states are computed, thereby encompassing the expected future costs, before addressing the terminal absorbing state of the OOS. Consequently, this approach facilitates more informed prepositioning decisions and helps avoid expensive emergency costs.

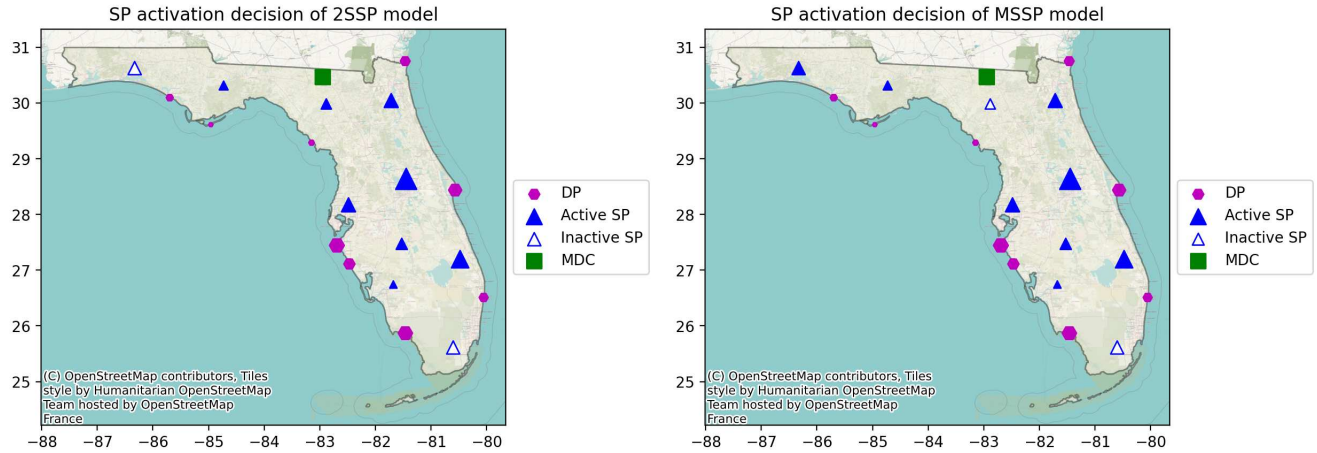

FIGURE 5 Activation of SPs in Ian case study for $\kappa^F = 5$, $\kappa^{PE} = 200$, $c^P = 5$.

This suggests that heuristic H1 is more cost-effective than H2 and substantially reduces the discrepancy between in-sample (training) and OOS (testing) results. Therefore, we opt to utilize heuristic H1 for the OOS test in the subsequent analyses.

TABLE 9 Selection of OOS heuristics in Hurricane Ian case study.

Approach	Average cost	Fixed	Inventory	Penalty	Emergency	Purchase	Transportation
In-sample	$2.75 \times 10^7 \pm 2.05 \times 10^5$	33%	7%	1%	3%	29%	27%
OOS-H1	$2.82 \times 10^7 \pm 1.39 \times 10^5$	33%	7%	1%	4%	28%	28%
OOS-H2	$4.07 \times 10^7 \pm 6.25 \times 10^5$	23%	5%	0%	34%	20%	19%

6.2.1 | OOS test performance

In this section, we discuss the performance of static and adaptive policies through OOS tests. Tables 10 and 11 present the results of these tests conducted on OOS scenarios from the MC model and true OOS scenarios, respectively. Notably, the SDDP algorithm terminates at the time limit in 12 out of 13 configurations. Consequently, the MSSP policies utilized in the OOS testing may not be the optimal policies.

Across all cost configurations, MSSP demonstrates a 7.01% higher cost efficiency than 2SSP-anticipative and a 40.26% higher efficiency than 2SSP-myopic for OOS scenarios generated from the MC model. Similarly, for true OOS scenarios, MSSP yields average cost savings of 6.63% and 41.99%, respectively. It is noteworthy that both OOS test results highlight the superior cost-saving capabilities of the MSSP model in the Ian case compared to the Florence case. This can be attributed to the variability in the landfall period observed in the sample paths, which benefits the adaptive decision-making process of relief prepositioning in the MSSP model.

The breakdown of cost components for each approach is detailed in Table 12. A notable distinction from the results in the Florence case is that the transportation costs (relief items and evacuees) constitute a higher percentage of the total cost. This can be attributed to the increased demand observed over a longer planning horizon and the more extensive logistics network in the Ian case study, where transportation emerges as a major cost factor.

Another significant difference lies in the 2SSP model, where the first-stage decision involves relief inventory and the start time of evacuation may vary across scenarios due to the different terminal stages in different scenarios. Consequently, a higher level of inventory is generally maintained in the 2SSP model to enhance the robustness of relief supply across all scenarios. However, such inventory management is less critical for MSSP, where relief inventory is treated as a state variable. Additionally, the higher relief inventory levels in the 2SSP model enable the avoidance of emergency transportation costs in 2SSP-anticipative, as it optimizes evacuation decisions with complete sample path information, resulting in a smaller proportion of emergency costs. However, inventory and purchase costs constitute a larger fraction of the total cost in 2SSP-anticipative

compared to MSSP, as observed in the base configuration results. Conversely, the emergency transportation emerges as a major cost component in 2SSP-myopic due to the myopic evacuation decisions made locally.

In contrast to the Florence case, where MSSP showed higher performance gap for OOS scenarios generated from the MC model compared to true OOS scenarios, the Ian case exhibits a consistent pattern of performance gap, with respect to 2SSP-anticipative, across both types of OOS scenarios. Specifically, the average costs for true OOS scenarios are slightly higher, with differences of 0.6%, 0.1%, and 4.2% for MSSP, 2SSP-anticipative, and 2SSP-myopic, respectively, compared to OOS scenarios from the MC model. In contrast, in the Florence case, these differences were 1.5%, 0.1%, and –1.0%. This suggests that the MC approximation in the Ian case performs better, possibly due to the more sophisticated modeling of uncertainty in hurricane position using cross- and track-errors instead of just one track-error as in the Florence case.

In the subsequent sections, our focus shifts to discussing the OOS test results obtained from true OOS scenarios, presented in the form of sensitivity analysis. It is worth noting that similar insights can be drawn for the test results on OOS scenarios generated from the MC model.

TABLE 10 OOS test results of Hurricane Ian case study on OOS scenarios from the MC model.

			MSSP	**2SSP-anticipative**		**2SSP-myopic**	
κ^F	κ^{PE}	c^P	**CI of obj**	**CI of obj**	**P-Gap**	**CI of obj**	**P-Gap**
5	200	5	$2.75 \times 10^7 \pm 1.01 \times 10^5$	$3.01 \times 10^7 \pm 9.88 \times 10^4$	8.74%	$5.25 \times 10^7 \pm 4.81 \times 10^5$	47.57%
1	200	5	$1.91 \times 10^7 \pm 9.31 \times 10^4$	$2.27 \times 10^7 \pm 8.92 \times 10^4$	15.87%	$4.78 \times 10^7 \pm 5.26 \times 10^5$	60.07%
10	200	5	$3.64 \times 10^7 \pm 1.07 \times 10^5$	$3.91 \times 10^7 \pm 9.88 \times 10^4$	6.66%	$6.13 \times 10^7 \pm 4.81 \times 10^5$	40.61%
20	200	5	$5.64 \times 10^7 \pm 1.11 \times 10^5$	$5.63 \times 10^7 \pm 1.12 \times 10^5$	-0.12%	$7.80 \times 10^7 \pm 4.74 \times 10^5$	27.70%
50	200	5	$1.01 \times 10^8 \pm 2.20 \times 10^5$	$1.01 \times 10^8 \pm 2.44 \times 10^5$	0.19%	$1.23 \times 10^8 \pm 5.47 \times 10^5$	17.86%
5	50	5	$2.63 \times 10^7 \pm 1.01 \times 10^5$	$2.87 \times 10^7 \pm 1.02 \times 10^5$	8.21%	$5.07 \times 10^7 \pm 4.69 \times 10^5$	48.08%
5	100	5	$2.75 \times 10^7 \pm 9.70 \times 10^4$	$2.97 \times 10^7 \pm 9.07 \times 10^4$	7.65%	$5.19 \times 10^7 \pm 4.76 \times 10^5$	47.10%
5	300	5	$2.86 \times 10^7 \pm 9.93 \times 10^4$	$3.04 \times 10^7 \pm 9.56 \times 10^4$	5.74%	$5.45 \times 10^7 \pm 5.17 \times 10^5$	47.51%
5	500	5	$2.91 \times 10^7 \pm 9.76 \times 10^4$	$3.05 \times 10^7 \pm 9.13 \times 10^4$	4.41%	$5.50 \times 10^7 \pm 5.18 \times 10^5$	46.99%
5	200	1	$1.90 \times 10^7 \pm 6.14 \times 10^4$	$1.95 \times 10^7 \pm 5.70 \times 10^4$	2.28%	$4.14 \times 10^7 \pm 4.48 \times 10^5$	54.02%
5	200	10	$3.82 \times 10^7 \pm 1.67 \times 10^5$	$4.33 \times 10^7 \pm 1.54 \times 10^5$	11.68%	$6.61 \times 10^7 \pm 5.26 \times 10^5$	42.13%
5	200	50	$1.15 \times 10^8 \pm 6.35 \times 10^5$	$1.39 \times 10^8 \pm 6.32 \times 10^5$	17.65%	$1.67 \times 10^8 \pm 9.81 \times 10^5$	31.49%
5	200	100	$1.63 \times 10^8 \pm 9.58 \times 10^5$	$1.66 \times 10^8 \pm 1.01 \times 10^6$	2.12%	$1.85 \times 10^8 \pm 1.07 \times 10^6$	12.18%

6.2.1.1 | *Sensitivity analysis on fixed cost*

The sensitivity analysis of fixed costs yields results consistent with those observed in the Florence case. When κ^F is low, a higher dominance of relief purchase and transportation costs is observed, as illustrated in Table 12. Consequently, the MSSP model benefits more from its adaptive decision-making capabilities. However, as κ^F increases, fixed costs become more dominant, diminishing the impact of adaptive decision-making on performance gap.

Given the longer planning horizon in the Ian case compared to the Florence case, the total keep-up cost of SPs is higher in the former. Interestingly, although fixed costs represent a smaller percentage of the total cost in the Ian case, this is counterbalanced by the higher percentage of penalty and transportation costs. With a higher demand observed over a longer planning horizon in the Ian case, penalty costs increase, particularly at high fixed costs.

6.2.1.2 | *Sensitivity analysis on penalty cost*

Similar to the Florence case results, the sensitivity analysis results of κ^{PE} indicate consistent outcomes within the selected range, with the average cost changing by less than 5% across all approaches. This aligns with the observation that penalty cost is less sensitive to the overall cost, and at high values of κ^{PE}, the MSSP model incurs zero penalty cost. As κ^{PE} increases, the penalty cost takes up a smaller percentage of the total cost, reflecting a trade-off with the emergency cost, which slightly increases. This suggests that while penalty cost gets more expensive, the combination of evacuee transportation and emergency relief supply is still relatively cheaper, representing a better trade-off decision.

6.2.1.3 | *Sensitivity analysis on purchase cost*

Similar to the observations in the Florence case, we find that the performance gap with respect to 2SSP-anticipative is lower when the purchase cost (c^P) is either at its lowest or highest values compared to configurations in between. As shown in Table 12, when the purchase cost is at its minimum value ($c^P = 1$), both MSSP and 2SSP-anticipative exhibit a growing

TABLE 11 OOS test results of Hurricane Ian case study on true OOS scenarios.

			MSSP	2SSP-anticipative		2SSP-myopic	
κ^F	κ^{PE}	c^P	CI of obj	CI of obj	P-Gap	CI of obj	P-Gap
5	200	5	$2.82 \times 10^7 \pm 1.39 \times 10^5$	$2.99 \times 10^7 \pm 1.43 \times 10^5$	5.91%	$5.35 \times 10^7 \pm 8.88 \times 10^5$	47.32%
1	200	5	$1.93 \times 10^7 \pm 1.25 \times 10^5$	$2.25 \times 10^7 \pm 1.26 \times 10^5$	14.25%	$4.91 \times 10^7 \pm 9.77 \times 10^5$	60.69%
10	200	5	$3.62 \times 10^7 \pm 1.46 \times 10^5$	$3.89 \times 10^7 \pm 1.66 \times 10^5$	7.03%	$6.18 \times 10^7 \pm 8.72 \times 10^5$	41.47%
20	200	5	$5.61 \times 10^7 \pm 1.49 \times 10^5$	$5.58 \times 10^7 \pm 2.15 \times 10^5$	-0.65%	$7.98 \times 10^7 \pm 9.11 \times 10^5$	29.67%
50	200	5	$9.99 \times 10^7 \pm 3.42 \times 10^5$	$1.01 \times 10^8 \pm 4.49 \times 10^5$	1.54%	$1.23 \times 10^8 \pm 9.64 \times 10^5$	19.11%
5	50	5	$2.60 \times 10^7 \pm 1.36 \times 10^5$	$2.87 \times 10^7 \pm 1.63 \times 10^5$	9.35%	$5.15 \times 10^7 \pm 8.52 \times 10^5$	49.43%
5	100	5	$2.75 \times 10^7 \pm 1.28 \times 10^5$	$2.97 \times 10^7 \pm 1.58 \times 10^5$	7.57%	$5.37 \times 10^7 \pm 8.89 \times 10^5$	48.88%
5	300	5	$2.86 \times 10^7 \pm 1.33 \times 10^5$	$3.02 \times 10^7 \pm 1.57 \times 10^5$	5.44%	$5.37 \times 10^7 \pm 8.94 \times 10^5$	46.85%
5	500	5	$2.94 \times 10^7 \pm 1.30 \times 10^5$	$3.03 \times 10^7 \pm 1.49 \times 10^5$	3.22%	$5.61 \times 10^7 \pm 9.61 \times 10^5$	47.64%
5	200	1	$1.90 \times 10^7 \pm 8.84 \times 10^4$	$1.96 \times 10^7 \pm 8.16 \times 10^4$	3.07%	$4.24 \times 10^7 \pm 8.43 \times 10^5$	55.26%
5	200	10	$3.75 \times 10^7 \pm 2.24 \times 10^5$	$4.26 \times 10^7 \pm 2.24 \times 10^5$	11.84%	$6.73 \times 10^7 \pm 9.55 \times 10^5$	44.24%
5	200	50	$1.14 \times 10^8 \pm 8.52 \times 10^5$	$1.35 \times 10^8 \pm 9.60 \times 10^5$	15.62%	$1.73 \times 10^8 \pm 1.63 \times 10^6$	34.05%
5	200	100	$1.69 \times 10^8 \pm 1.44 \times 10^6$	$1.73 \times 10^8 \pm 1.52 \times 10^6$	1.93%	$2.15 \times 10^8 \pm 1.72 \times 10^6$	21.26%

TABLE 12 Proportion of cost components, on average, of OOS test on true OOS scenarios in Hurricane Ian case study.

			Fixed			Inventory			Penalty			Emergency			Relief Purchase			Transportation		
κ^F	κ^{PE}	c^P	MS	2-A	2-M	MS	2-A	2-M	MS	2-A	2-M	MS	2-A	2-M	MS	2-A	2-M	MS	2-A	2-M
5	200	5	33%	30%	17%	7%	9%	5%	1%	2%	1%	4%	1%	44%	28%	34%	19%	28%	25%	15%
1	200	5	11%	9%	4%	10%	11%	6%	0%	0%	0%	4%	2%	54%	40%	46%	21%	35%	32%	15%
10	200	5	49%	44%	28%	5%	6%	4%	2%	3%	2%	3%	1%	37%	21%	26%	16%	19%	20%	13%
20	200	5	65%	58%	41%	3%	4%	3%	1%	6%	4%	4%	0%	29%	14%	18%	13%	14%	13%	10%
50	200	5	73%	66%	54%	2%	2%	2%	10%	16%	13%	1%	0%	17%	7%	9%	7%	7%	7%	6%
5	50	5	31%	24%	14%	7%	8%	4%	5%	12%	7%	1%	0%	43%	29%	33%	18%	27%	24%	14%
5	100	5	34%	27%	15%	7%	9%	5%	1%	5%	3%	3%	1%	43%	28%	34%	19%	27%	24%	15%
5	300	5	36%	30%	17%	7%	9%	5%	0%	3%	2%	4%	1%	44%	27%	34%	19%	26%	25%	14%
5	500	5	37%	30%	16%	7%	9%	4%	0%	1%	1%	5%	2%	46%	27%	34%	18%	24%	25%	14%
5	200	1	47%	46%	21%	2%	3%	1%	3%	3%	1%	3%	0%	53%	8%	11%	5%	37%	38%	18%
5	200	10	24%	21%	13%	10%	11%	7%	1%	1%	1%	3%	3%	37%	41%	47%	30%	20%	17%	11%
5	200	50	8%	6%	5%	13%	12%	10%	9%	12%	6%	4%	14%	29%	60%	50%	45%	6%	5%	5%
5	200	100	3%	1%	1%	4%	1%	2%	70%	83%	59%	6%	14%	36%	15%	0%	0%	1%	1%	1%

dominance of transportation and fixed costs. This dominance underscores a high rate of relief items purchase and evacuation. Even in the static 2SSP model, there is effective pre-positioning of relief logistics with a sufficient inventory level, ensuring robustness to accommodate demand for most hurricane scenarios. Moreover, leveraging the complete sample-path information in 2SSP-anticipative facilitates evacuation optimization, leading to minimized penalties and emergency costs through adequate provisioning of relief inventory. The adaptability advantage of the MSSP model diminishes under these conditions, resulting in a decreased performance gap compared to when $c^P = 10$.

Similarly, as the purchase cost increases to its maximum value ($c^P = 100$), the pre-positioning of relief items becomes more expensive, leading to a higher frequency of local penalties and emergency costs incurred to meet demand in both MSSP and 2SSP-anticipative. With the non-adaptive inventory state variables in 2SSP-anticipative, paying emergency cost locally appears to be more cost-effective than the regular procurement and inventory costs for relief items spanning multiple periods. Consequently, the performance gap with respect to 2SSP-anticipative becomes lower. However, at $c^P = 10$ or 50, MSSP efficiently satisfies demand through inventory rather than emergency costs, despite the higher relief commodity purchase cost.

Meanwhile, for 2SSP-myopic, which lacks foresight into future demand information, the corresponding solution involves evacuation carried out with emergency costs, which is more cost-effective than incurring local penalty costs. Consequently, emergency costs emerge as the dominant factor, leading to an increase in the performance gap with respect to 2SSP-myopic.

7 | CONCLUSION AND FUTURE RESEARCH

In this paper, we have studied an integrated problem of hurricane evacuation and relief logistics planning under the evolving uncertainty of hurricane attributes. The main advantage for a decision maker to integrate these two operations is that efficient

propositioning decisions can be made depending on the evacuation decisions which are unknown initially. We have demonstrated an approach to model the time-dependent forecast uncertainty using historical errors using the AR–1 model, integrate it with a point forecast of the hurricane's trajectory (intensity and track) to generate hurricane scenarios, and approximate the hurricane process as a Markov chain model using the generated scenarios for the proposed MSSP model. We have conducted two case studies, on Hurricane Florence and Hurricane Ian in South Carolina and Florida respectively, and considered deterministic and random landfall times in these studies. Our extensive numerical experiments on OOS scenarios have demonstrated the effectiveness of the fully adaptive MSSP model in terms of minimizing the expected overall cost, despite their computational challenges compared to the 2SSP model in both cases. Specifically, the MSSP model has exhibited higher cost efficiency in the random landfall time case compared to the deterministic case, showcasing its effectiveness in these more complex settings.

In our model, we have limited the SP activation decisions to the first stage only mainly because of the additional computational complexity that would be introduced once we make these decisions adaptive as well. One future research direction is to consider a fully adaptive mixed-integer MSSP model with adaptive decisions of SP activation as the hurricane attributes unfold. Additionally, our model treats the allocations of evacuees from DPs to SPs as decision variables. However, in practice, evacuees subject to evacuation orders may not adhere to the model's prescribed decisions and opt to evacuate independently. This scenario can be modeled as a bi-level optimization problem. At the upper level, decisions regarding SP activation and evacuee flow are made, while at the lower level, the number of evacuees adhering to specific routes under a hurricane scenario is determined. A relevant study by [29] addresses a similar problem, employing a two-stage location allocation model at the upper level and incorporating travel time and volume considerations in the lower level. Furthermore, our model estimates demand by assuming that evacuees voluntarily seek public shelters. However, in reality, mandatory evacuation orders may be issued by state agencies, altering the demand dynamics. This consideration motivates the development of novel MSSP models with decision-dependent uncertainty.

ACKNOWLEDGMENTS

The authors acknowledge partial support by the National Science Foundation [Grant CMMI 2045744]. Any opinions, findings, and conclusions or recommendations expressed in this material are those of the authors and do not necessarily reflect the views of the National Science Foundation.

CONFLICT OF INTEREST

The authors declare no potential conflict of interests.

REFERENCES

1. *ANNEX H TO HURRICANE PLAN GENERAL POPULATION AND SHELTER MANAGEMENT*, https://www.scemd.org/media/1323/annex-h-general-population-shelter-management.pdf Accessed: 2024-02-02.
2. *How to read the forecast/advisory*, https://www.nhc.noaa.gov/help/tcm.shtml Accessed: 2023-11-13.
3. *National hurricane center tropical cyclone report: Hurricane ian*, https://www.nhc.noaa.gov/data/tcr/AL092022_Ian.pdf Accessed: 2023-11-13.
4. *Statewide emergency shelter plans*, https://www.floridadisaster.org/dem/response/infrastructure/statewide-emergency-shelter-plan/ Accessed: 2023-11-13.
5. *National hurricane center forecast verification*, https://www.nhc.noaa.gov/verification/verify7.shtml (2022). Accessed: 2023-02-04.
6. *Sheltering During Hurricanes, Centers for Disease Control and Prevention*, https://www.cdc.gov/nceh/hsb/disaster/sheltering-during_hurricanes.html (2022). Accessed: 2023-01-30.
7. M. Akbarpour, S. A. Torabi, and A. Ghavamifar, *Designing an integrated pharmaceutical relief chain network under demand uncertainty*, Transportation research part e: logistics and transportation review **136** (2020), 101867.
8. D. Alem, A. Clark, and A. Moreno, *Stochastic network models for logistics planning in disaster relief*, European Journal of Operational Research **255** (2016), no. 1, 187–206.
9. P. Apivatanagul, R. A. Davidson, and L. K. Nozick, *Bi-level optimization for risk-based regional hurricane evacuation planning*, Natural Hazards **60** (2012), 567–588.
10. E. J. Baker, *Hurricane evacuation behavior*, International Journal of Mass Emergencies & Disasters **9** (1991), no. 2, 287–310.
11. V. Bayram and H. Yaman, *A stochastic programming approach for shelter location and evacuation planning*, RAIRO-Operations Research-Recherche Opérationnelle **52** (2018), no. 3, 779–805.
12. G. E. Box, G. M. Jenkins, G. C. Reinsel, and G. M. Ljung, *Time series analysis: forecasting and control*, John Wiley & Sons, 2015.
13. L. Bucci, L. Alaka, A. Hagen, S. Delgado, and J. Beven, *National hurricane center tropical cyclone report* (2023).
14. J. M. Chambers, *Graphical methods for data analysis*, CRC Press, 2018.
15. Y. Chang, Y. Song, and B. Eksioglu, *A stochastic look-ahead approach for hurricane relief logistics operations planning under uncertainty*, Annals of Operations Research (2021), 1–33.
16. I. Cohen et al., *Pearson correlation coefficient*, Noise reduction in speech processing (2009), 1–4.
17. J. Dalal and H. Üster, *Combining worst case and average case considerations in an integrated emergency response network design problem*, Transportation Science **52** (2018), no. 1, 171–188.
18. R. A. Davidson et al., *An integrated scenario ensemble-based framework for hurricane evacuation modeling: Part 1 – decision support system*, Risk analysis **40** (2020), no. 1, 97–116.

19. L. Ding, S. Ahmed, and A. Shapiro, *A python package for multi-stage stochastic programming*, Optimization online (2019), 1–42.
20. O. Dowson, *The policy graph decomposition of multistage stochastic programming problems*, Networks **76** (2020), no. 1, 3–23.
21. D. Duque, H. Yang, and D. Morton, *Optimizing diesel fuel supply chain operations for hurricane relief*, Optim. Online (2020).
22. G. Erbeyoğlu and Ü. Bilge, *A robust disaster preparedness model for effective and fair disaster response*, European Journal of Operational Research **280** (2020), no. 2, 479–494.
23. M. Fattahi and K. Govindan, *Data-driven rolling horizon approach for dynamic design of supply chain distribution networks under disruption and demand uncertainty*, Decision Sciences **53** (2022), no. 1, 150–180.
24. C. for Disease Control and P. (CDC), *Evacuating during hurricanes*, https://www.cdc.gov/nceh/hsb/disaster/evacuating-during_hurricanes.html (2023). Accessed: 2023-11-12.
25. M. Goerigk, K. Deghdak, and P. Heßler, *A comprehensive evacuation planning model and genetic solution algorithm*, Transportation research part E: logistics and transportation review **71** (2014), 82–97.
26. J. A. Hartigan and M. A. Wong, *Algorithm as 136: A k-means clustering algorithm*, Journal of the royal statistical society. series c (applied statistics) **28** (1979), no. 1, 100–108.
27. P. Kall, S. W. Wallace, and P. Kall, *Stochastic programming*, vol. 5, Springer, 1994.
28. J. Kruger, *Hurricane evacuation laws in eight southern us coastal statesdecember 2018*, MMWR. Morbidity and Mortality Weekly Report **69** (2020).
29. A. C. Li, N. Xu, L. Nozick, and R. Davidson, *Bilevel optimization for integrated shelter location analysis and transportation planning for hurricane events*, Journal of Infrastructure Systems **17** (2011), no. 4, 184–192.
30. B. Liang, D. Yang, X. Qin, and T. Tinta, *A risk-averse shelter location and evacuation routing assignment problem in an uncertain environment*, International journal of environmental research and public health **16** (2019), no. 20, 4007.
31. G. J. Lim, S. Zangeneh, M. R. Baharnemati, and T. Assavapokee, *A capacitated network flow optimization approach for short notice evacuation planning*, European Journal of Operational Research **223** (2012), no. 1, 234–245.
32. E. J. Lodree Jr, K. N. Ballard, and C. H. Song, *Pre-positioning hurricane supplies in a commercial supply chain*, Socio-Economic Planning Sciences **46** (2012), no. 4, 291–305.
33. N. Löhndorf and A. Shapiro, *Modeling time-dependent randomness in stochastic dual dynamic programming*, European Journal of Operational Research **273** (2019), no. 2, 650–661.
34. R. Pasch, R. Berg, D. Roberts, and P. Papin, *National hurricane center tropical cyclone report hurricane laura (al132020)* (2020).
35. M. V. Pereira and L. M. Pinto, *Multi-stage stochastic optimization applied to energy planning*, Mathematical programming **52** (1991), 359–375.
36. A. B. Philpott and Z. Guan, *On the convergence of stochastic dual dynamic programming and related methods*, Operations Research Letters **36** (2008), no. 4, 450–455.
37. W. B. Powell, *Reinforcement Learning and Stochastic Optimization: A unified framework for sequential decisions*, John Wiley & Sons, 2022.
38. T. Rambha, L. K. Nozick, and R. Davidson, *Modeling hurricane evacuation behavior using a dynamic discrete choice framework*, Transportation research part B: methodological **150** (2021), 75–100.
39. E. Regnier and P. A. Harr, *A dynamic decision model applied to hurricane landfall*, Weather and Forecasting **21** (2006), no. 5, 764–780.
40. S. Rezapour, R. Z. Farahani, and N. Morshedlou, *Impact of timing in post-warning prepositioning decisions on performance measures of disaster management: a real-life application*, European Journal of Operational Research **293** (2021), no. 1, 312–335.
41. M. Sabbaghtorkan, R. Batta, and Q. He, *Prepositioning of assets and supplies in disaster operations management: Review and research gap identification*, European Journal of Operational Research **284** (2020), no. 1, 1–19.
42. A. Shapiro, *Tutorial on risk neutral, distributionally robust and risk averse multistage stochastic programming*, European Journal of Operational Research **288** (2021), no. 1, 1–13.
43. A. Shapiro, D. Dentcheva, and A. Ruszczynski, *Lectures on stochastic programming: modeling and theory*, SIAM, 2021.
44. J. Shu, M. Song, B. Wang, J. Yang, and S. Zhu, *Humanitarian relief network design: Responsiveness maximization and a case study of typhoon rammasun*, IISE Transactions **55** (2023), no. 3, 301–313.
45. M. Siddig and Y. Song, *Multi-stage stochastic programming methods for adaptive disaster relief logistics planning*, arXiv preprint arXiv:2201.10678 (2022).
46. H. Üster and J. Dalal, *Strategic emergency preparedness network design integrating supply and demand sides in a multi-objective approach*, IISE Transactions **49** (2017), no. 4, 395–413.
47. G. A. Velasquez, M. E. Mayorga, and O. Y. Özaltın, *Prepositioning disaster relief supplies using robust optimization*, IISE Transactions **52** (2020), no. 10, 1122–1140.
48. D. Wang, K. Yang, and L. Yang, *Risk-averse two-stage distributionally robust optimisation for logistics planning in disaster relief management*, International Journal of Production Research **61** (2023), no. 2, 668–691.
49. L. Wang, *A two-stage stochastic programming framework for evacuation planning in disaster responses*, Computers & Industrial Engineering **145** (2020), 106458.
50. L. Wang, L. Yang, Z. Gao, S. Li, and X. Zhou, *Evacuation planning for disaster responses: A stochastic programming framework*, Transportation research part C: emerging technologies **69** (2016), 150–172.
51. X. J. Wang and J. A. Paul, *Robust optimization for hurricane preparedness*, International Journal of Production Economics **221** (2020), 107464.
52. B. Zahiri, S. A. Torabi, M. Mohammadi, and M. Aghabegloo, *A multi-stage stochastic programming approach for blood supply chain planning*, Computers & Industrial Engineering **122** (2018), 1–14.
53. J. Zou, S. Ahmed, and X. A. Sun, *Stochastic dual dynamic integer programming*, Mathematical Programming **175** (2019), 461–502.

□

APPENDIX

A ADDITIONAL TABLES AND FIGURES

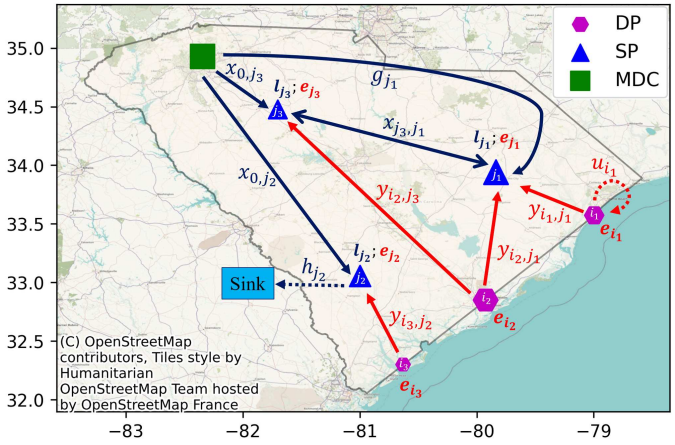

FIGURE A1 An illustration of decision variables on an example network with $|I| = |J| = 3$. Node "sink" is a dummy node for shipping out the unused relief items from SPs, which is used in the flow balance constraints defined at the SPs. The decision variable u_{i_1} is defined in a self-loop at i_1 to indicate the unmet demand at t which can be accounted for at $t + 1$.

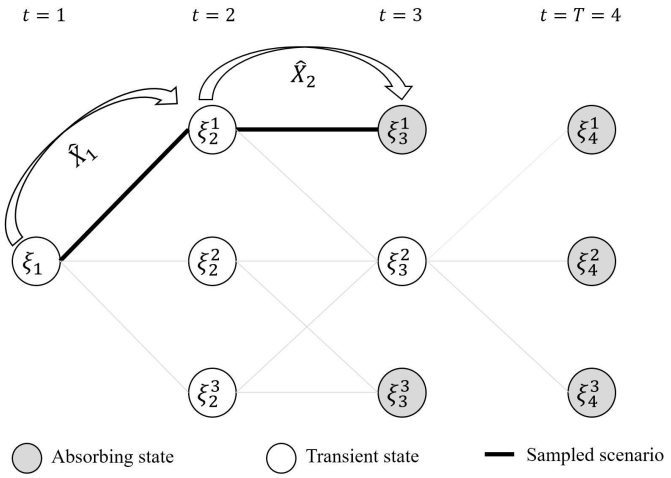

FIGURE A2 Illustration of the forward pass of the SDDP algorithm.

TABLE A1 Estimated AR–1 parameters from historical data using the maximum likelihood estimation.

Parameters	Along	Cross	Track	Intensity
ρ_{mle}	1.12	1.09	1.05	0.98
σ_{mle}	39.12	33.18	0.38	8.03

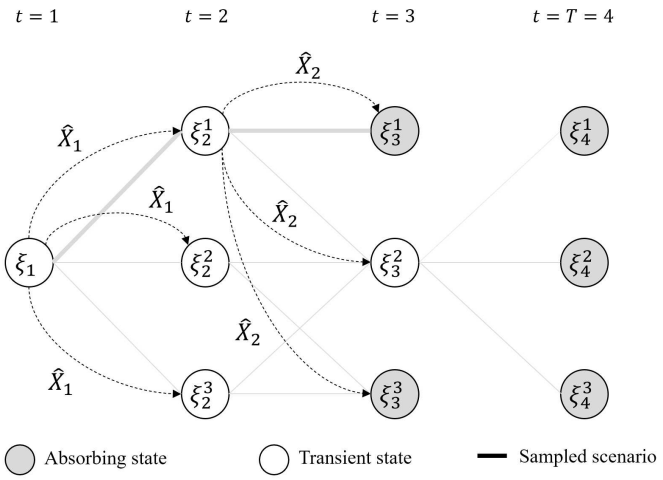

FIGURE A3 Solving stage-t problems with $\hat{X}_{t-1}$ in the backward pass of the SDDP algorithm.

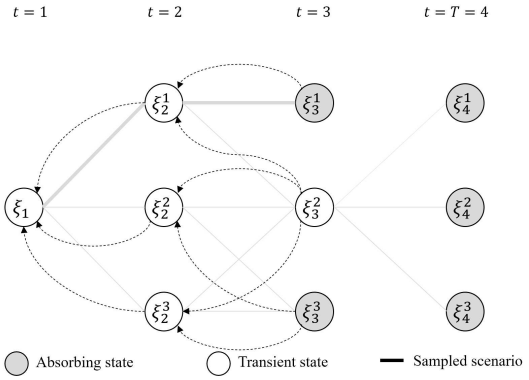

FIGURE A4 An illustration of cut sharing in the backward pass of the SDDP algorithm.

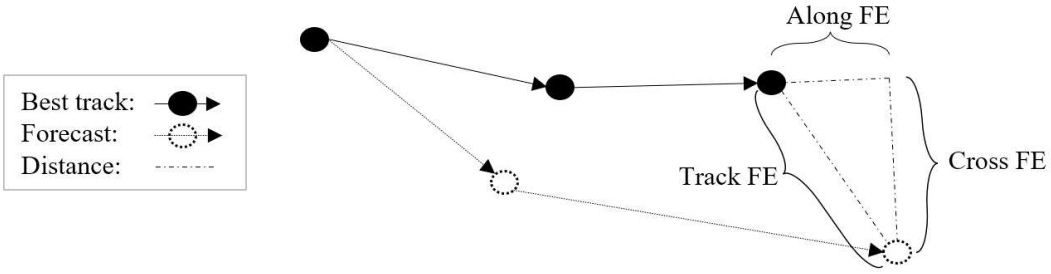

FIGURE A5 An illustration of track FEs.

TABLE A2 Pearson correlation coefficients for different types of FEs at various forecast lead times.

Hours	012	024	036	048	072	096	120
Track-Intensity FE	0.005	0.02	0.03	0.017	-0.01	-0.065	-0.056
Along-Cross FE	0.021	0.041	0.065	0.112	0.058	-0.046	-0.075

TABLE A3 Number of Markovian states at each period for the Hurricane Florence case study. For each period t: S_t^T is the number of track states at t, S_t^I is the number of intensity states, and $\mathbf{S_t} = \mathbf{S_t^T} \times \mathbf{S_t^I}$.

Hours	000	012	024	036	048	060	072	084	096	108	120
$\mathbf{S_t^T}$	1	2	4	4	5	6	7	9	11	14	15
$\mathbf{S_t^I}$	1	6	6	6	6	6	6	6	6	6	6
$\mathbf{S_t}$	1	12	24	24	30	36	42	54	66	84	90

TABLE A4 Number of Markovian states at each period for the Hurricane Ian case study. For each period t: S_t^A and S_t^C are the number of along and cross states at t, respectively, S_t^I is the number of intensity states, and $\mathbf{S_t} = \mathbf{S_t^A} \times \mathbf{S_t^C} \times \mathbf{S_t^I}$.

Hours	000	012	024	036	048	060	072	084	096	108	120	132	144	156	168
$\mathbf{S_t^A}$	1	2	2	3	3	3	3	3	4	4	4	5	5	5	5
$\mathbf{S_t^C}$	1	2	3	3	3	3	4	4	4	4	5	5	5	5	5
$\mathbf{S_t^I}$	1	6	6	6	6	6	6	6	6	6	6	6	6	6	6
$\mathbf{S_t}$	1	24	36	54	54	54	72	72	72	72	120	150	150	150	150

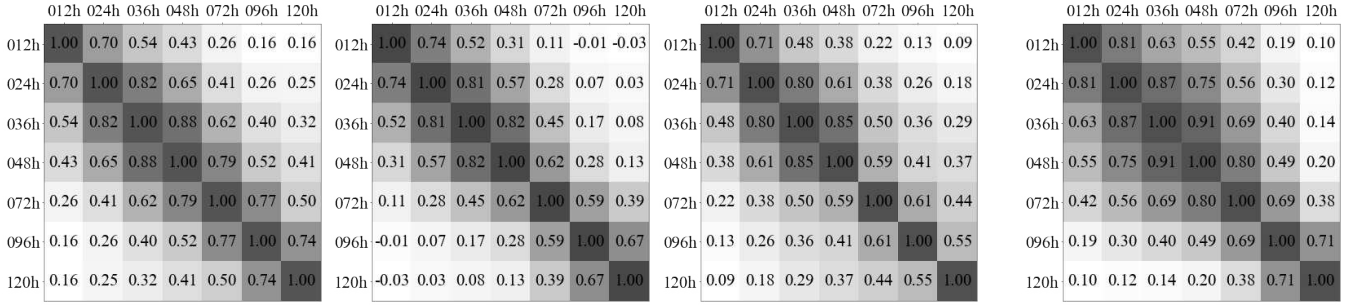

(a) Track error (b) Intensity error (c) Along error (d) Cross error

FIGURE A6 Pearson correlation coefficients between FEs at various forecast lead times from historical data.

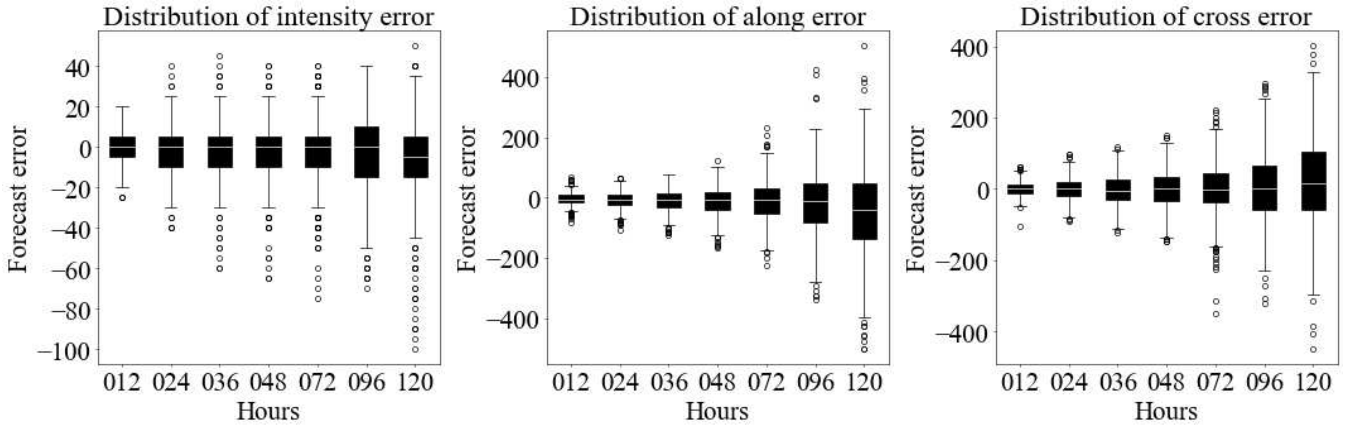

(a) Intensity error (b) Along error (c) Cross error

FIGURE A7 The FE distribution estimated from historical data.

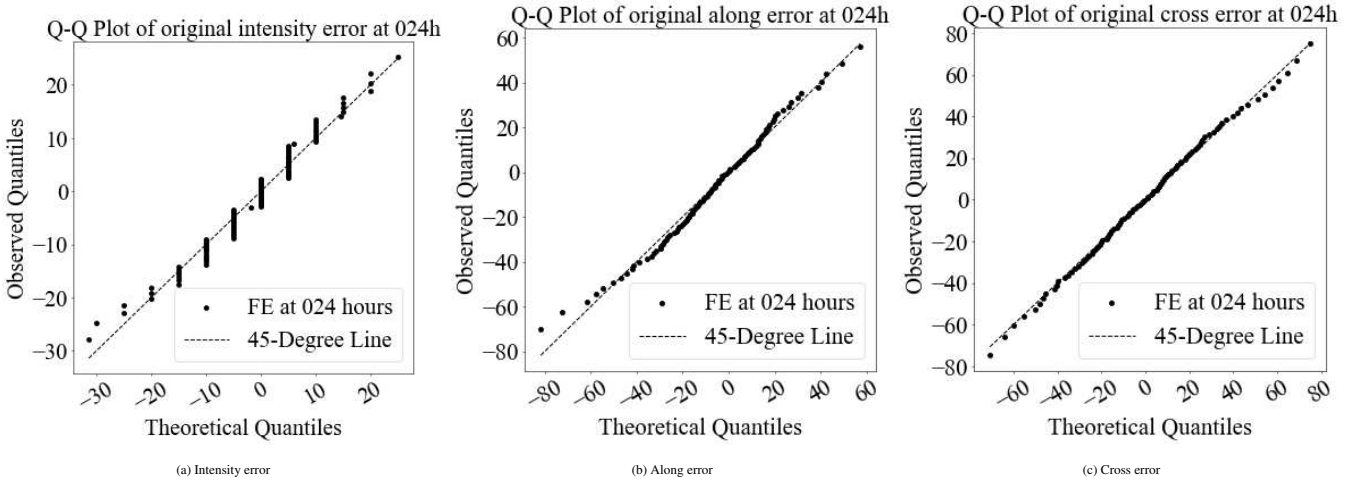

(a) Intensity error (b) Along error (c) Cross error

FIGURE A8 Quantile-Quantile plots of various types of FEs at 024 hours.

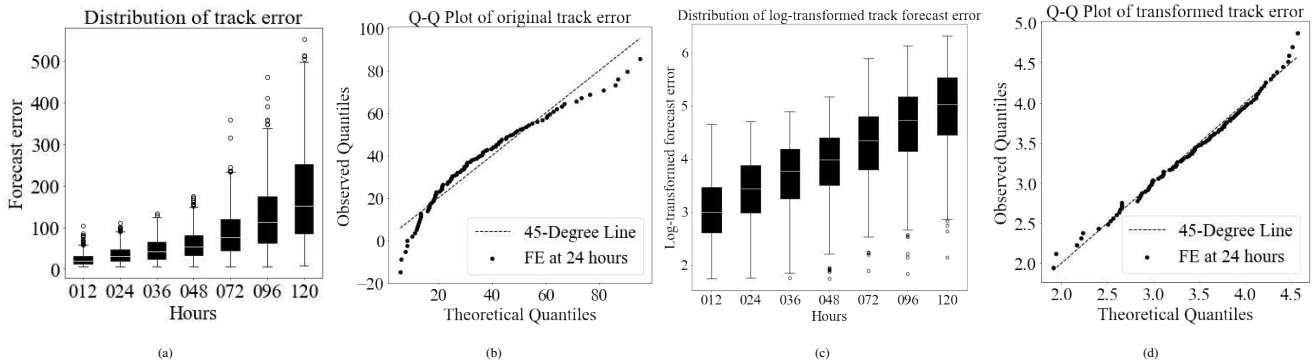

FIGURE A9 Track error distribution and Q-Q plots at 024*h*.

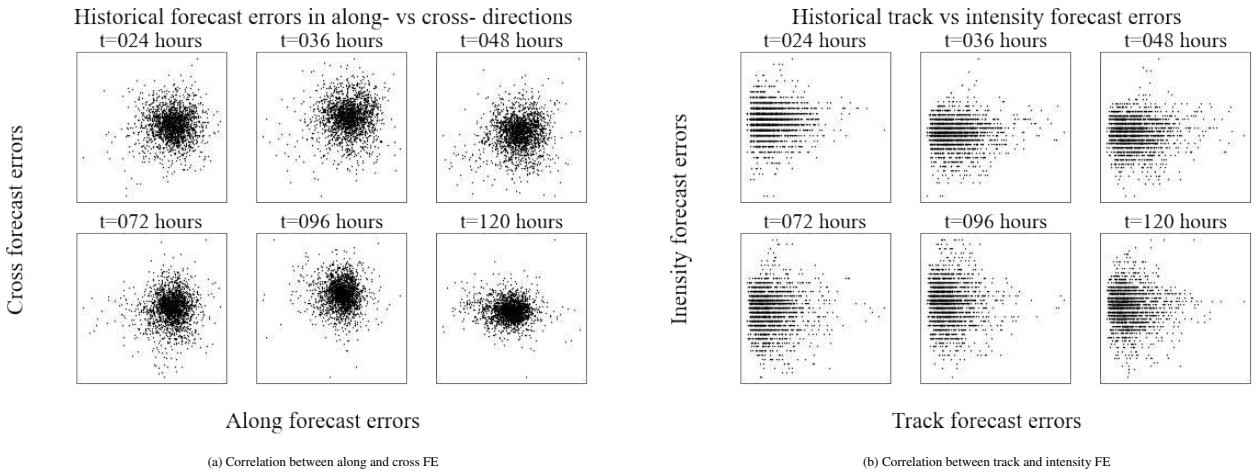

(a) Correlation between along and cross FE

(b) Correlation between track and intensity FE

FIGURE A10 Correlation between different FEs.

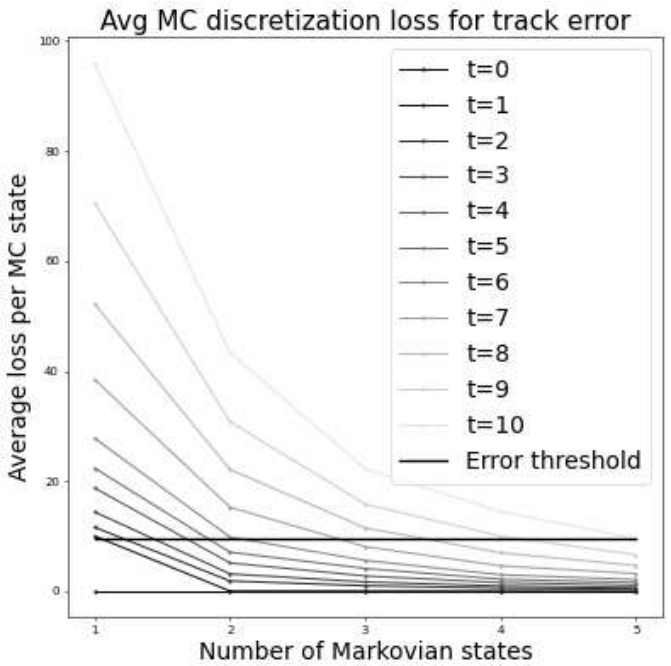

FIGURE A11 An example of the number of Markovian states to use per period based on a given MC discretization error threshold.

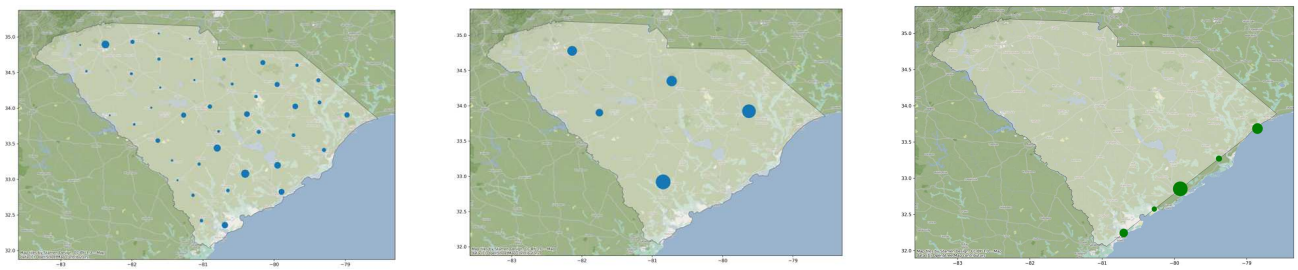

(a) Shelters at county level

(b) Clustered candidate shelters

(c) Clustered demand points

FIGURE A12 Illustration of SPs in the Hurricane Florence case study.